

Accepted Manuscript

^{18}F -Labeled indole-based analogs as highly selective radioligands for imaging sigma-2 receptors in the brain

Liang Wang, Jiajun Ye, Yingfang He, Winnie Deuther-Conrad, Jinming Zhang, Xiaojun Zhang, Mengchao Cui, Jörg Steinbach, Yiyun Huang, Peter Brust, Hongmei Jia

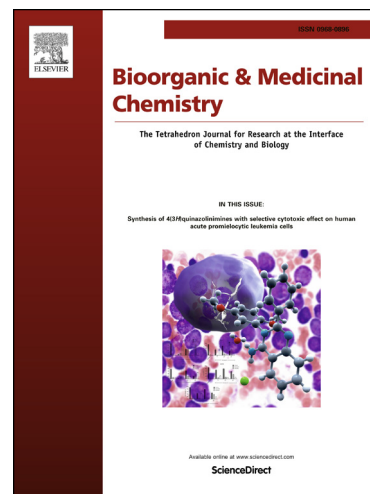
PII: S0968-0896(17)30681-8
DOI: <http://dx.doi.org/10.1016/j.bmc.2017.05.019>
Reference: BMC 13737

To appear in: *Bioorganic & Medicinal Chemistry*

Received Date: 31 March 2017
Accepted Date: 8 May 2017

Please cite this article as: Wang, L., Ye, J., He, Y., Deuther-Conrad, W., Zhang, J., Zhang, X., Cui, M., Steinbach, J., Huang, Y., Brust, P., Jia, H., ^{18}F -Labeled indole-based analogs as highly selective radioligands for imaging sigma-2 receptors in the brain, *Bioorganic & Medicinal Chemistry* (2017), doi: <http://dx.doi.org/10.1016/j.bmc.2017.05.019>

This is a PDF file of an unedited manuscript that has been accepted for publication. As a service to our customers we are providing this early version of the manuscript. The manuscript will undergo copyediting, typesetting, and review of the resulting proof before it is published in its final form. Please note that during the production process errors may be discovered which could affect the content, and all legal disclaimers that apply to the journal pertain.



^{18}F -Labeled indole-based analogs as highly selective radioligands for imaging sigma-2 receptors in the brain

Liang Wang^a, Jiajun Ye^a, Yingfang He^a, Winnie Deuther-Conrad^b, Jinming Zhang^c, Xiaojun Zhang^c, Mengchao Cui^{a,*}, Jörg Steinbach^b, Yiyun Huang^d, Peter Brust^b, Hongmei Jia^{a,*}

^aKey Laboratory of Radiopharmaceuticals (Beijing Normal University), Ministry of Education, College of Chemistry, Beijing Normal University, Beijing 100875, China

^bHelmholtz-Zentrum Dresden-Rossendorf, Institute of Radiopharmaceutical Cancer Research/ Department of Neuroradiopharmaceuticals, 04318 Leipzig, Germany

^cNuclear Medicine Department, Chinese PLA General Hospital, Beijing 100853, China

^dPET Center, Department of Radiology and Biomedical Imaging, Yale University, New Haven, CT, USA

*Corresponding author. Tel.: 86-10-58808891. Fax: 86-10-58808891. E-mail address: hmjia@bnu.edu.cn, cmc@bnu.edu.cn

ABSTRACT

We have designed and synthesized a series of indole-based σ_2 receptor ligands containing 5,6-dimethoxyisoindoline or 6,7-dimethoxy-1,2,3,4-tetrahydroisoquinoline as pharmacophore. *In vitro* competition binding assays showed that all ten ligands possessed low nanomolar affinity ($K_i = 1.79\text{--}5.23$ nM) for σ_2 receptors and high subtype selectivity ($K_i(\sigma_2)/K_i(\sigma_1) = 56\text{--}708$). Moreover, they showed high selectivity for σ_2 receptor over the vesicular acetylcholine transporter (>1000-fold). The corresponding radiotracers [^{18}F]16 and [^{18}F]21 were prepared by an efficient one-pot, two-step reaction sequence with a home-made automated synthesis module, with 10–15% radiochemical yield and radiochemical purity of >99%. Both radiotracers showed high brain uptake and σ_2 receptor binding specificity in mice.

Keywords: sigma-2 receptors; ^{18}F ; indole-based analogs; brain

1. INTRODUCTION

The sigma-2 (σ_2) receptor (molecular weight ~ 21.5 kDa¹) is believed to play important roles in the regulation of cellular differentiation.² It has been shown to be upregulated in various types of tumor cells,³⁻⁷ with approximately 10-fold higher expression in proliferating than quiescent tumors.⁸⁻¹⁰ Thus the σ_2 receptor has been suggested to be a biomarker for the proliferative status of solid tumors.¹¹⁻¹² Moreover, the σ_2 receptor interacts with Ca²⁺ channels and participates in various central nervous system (CNS) processes,¹³⁻¹⁵ with potential impact on learning and memory.¹⁶ Hence it is also considered a therapeutic target for the treatment of brain disorders.¹⁷⁻¹⁹

Over the years, substantial efforts have been directed toward the development of *in vivo* imaging agents for the investigation of σ_2 receptors in human diseases.¹¹⁻¹² However, up to date,

N-{4-[6,7-dimethoxy-3,4-dihydroisoquinolin-2(1*H*)-yl]butyl}-2-(2-[¹⁸F]fluoroethoxy)-5-methylbenzamide ([¹⁸F]ISO-1) is the only radiotracer that has been tested in humans for tumor imaging.²⁰⁻²² [¹⁸F]ISO-1 showed high uptake and clear visualization of EMT-6 tumors in female Balb/c mice. However, it is less suitable for imaging σ_2 receptors in the brain due to its low brain uptake ($\sim 0.76\%$ injected dose (ID)/g at 2 min).²⁰ Our aim was to develop radioligands with high affinity for σ_2 receptors, good selectivity, high uptake and favorable kinetics for use in brain imaging.

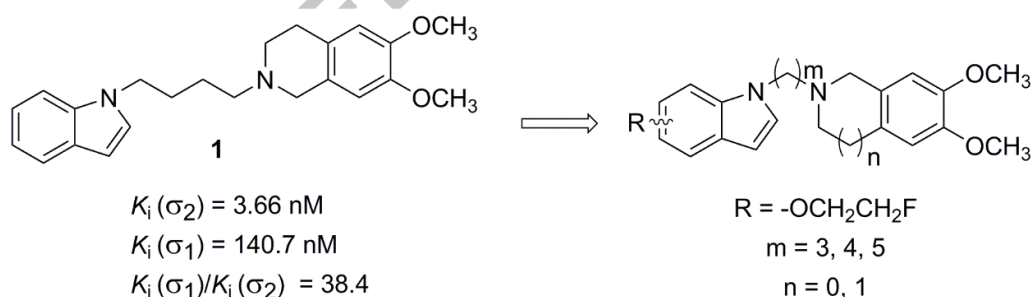


Figure 1. Design concept for the indole-based compounds.

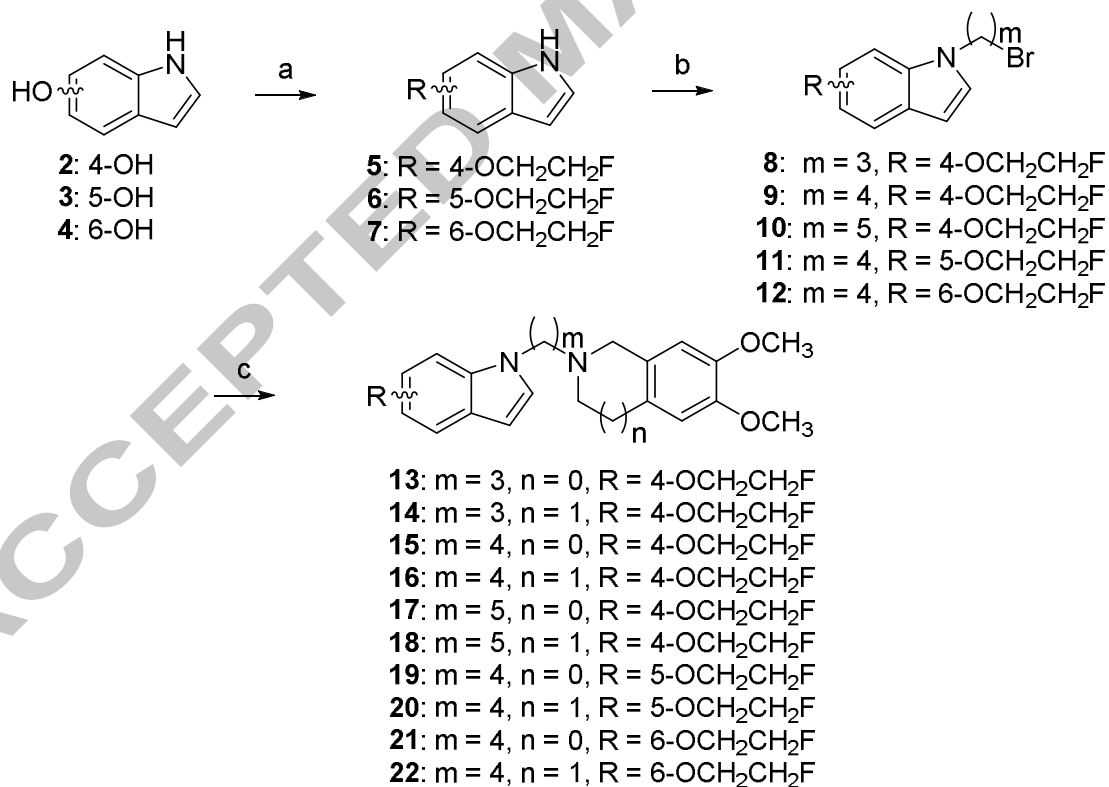
2-[4-(indol-1-yl)butyl]-6,7-dimethoxy-1,2,3,4-tetrahydroisoquinoline²³ (**1**, **Figure 1**) was reported to have nanomolar affinity and acceptable selectivity for σ_2 receptors, and hence chosen as the lead compound to design a series of indole-based derivatives. The design concept is shown in **Figure 1**. At first, a fluoroethoxy group was introduced at different positions of the indole ring to enable the incorporation of ¹⁸F for PET imaging. Second, the length of the carbon chain between the indole ring and the

6,7-dimethoxy-1,2,3,4-tetrahydroisoquinoline moiety was modified to explore the linker effect on pharmacokinetic properties of the compounds. Finally, the 6,7-dimethoxy-1,2,3,4-tetrahydroisoquinoline moiety was replaced by another σ_2 -preferring 5,6-dimethoxyisoindoline moiety to lower the lipophilicity. Herein we report the synthesis of these novel indole-based derivatives, together with the ^{18}F -labeled radiotracers [^{18}F]**16** and [^{18}F]**21** and their evaluation for imaging σ_2 receptors in the brain.

2. RESULTS

2.1 Chemistry.

The synthetic routes for the indole-based derivatives **13–22** are depicted in **Scheme 1**. Intermediates **5–7** were obtained by reaction of the hydroxyindols **2–4** with 1-bromo-2-fluoroethane under basic conditions. Based on a recently reported method,²³ *N*-alkylation of compounds **5–7** with the corresponding bromide provided compounds **8–12**. Subsequent reaction with 6,7-dimethoxy-1,2,3,4-tetrahydroisoquinoline or 5,6-dimethoxyisoindoline then afforded compounds **13–22** in yields of 34–94%.



Scheme 1. Reagents and conditions: (a) 1-bromo-2-fluoroethane, CH₃CN, K₂CO₃, 90 °C, 6 h, for **5**, 92%, for **6**, 69%, and for **7**, 70%; (b) DMF, KOH, Br(CH₂)_mBr, TBAF, r.t, 2 h, 24–82%;

(c) CH₃CN, 6,7-dimethoxy-1,2,3,4-tetrahydroisoquinoline/5,6-dimethoxyisoindoline, K₂CO₃, 90 °C, 6 h, 34–94%.

The target compounds were characterized by ¹H NMR, ¹³C NMR and high-resolution mass spectrometry (HRMS). Chemical purities of ≥ 95% were identified by high performance liquid chromatography (HPLC) analysis (see Supporting Information).

Table 1. Binding affinities of indole-based compounds^a

Compd	m	n	Position of OCH ₂ CH ₂ F	K _i (σ ₁) (nM)	K _i (σ ₂) (nM)	K _i (σ ₁)/ K _i (σ ₂)	K _i (VACHT) (nM)	K _i (VACHT)/ K _i (σ ₂)
1^b	4	1	-	140.7 ± 5.7	3.66 ± 0.83	38.4	-	-
13	3	0	4-	270 ± 17	4.51 ± 0.33	59.9	-	-
14	3	1	4-	293 ± 6	5.23 ± 0.57	56.0	-	-
15	4	0	4-	371 ± 105	1.79 ± 0.86	207.5	34280 ± 8443	19151
16	4	1	4-	1698 ± 548	2.40 ± 0.58	707.7	3570 ± 88	1488
17	5	0	4-	426 ± 54	3.28 ± 0.18	129.8	-	-
18	5	1	4-	262 ± 134	2.82 ± 0.67	92.7	-	-
19	4	0	5-	187 ± 1.41	3.27 ± 0.19	57.6	-	-
20	4	1	5-	471 ± 107	2.74 ± 0.17	172.1	36865 ± 205	13454
21	4	0	6-	376 ± 351	2.63 ± 0.48	143.2	35355 ± 7729	13443
22	4	1	6-	263 ± 107	3.24 ± 0.21	81.3	-	-
Haloperidol				4.95 ± 1.74	20.7 ± 0.07	4.2	-	-

^aValues are the mean ± standard deviation (SD) of at least two experiments performed in triplicate. ^bFrom reference²³.

2.2 *In Vitro* Radioligand Competition Binding Assays.

The affinities of compounds **13–22** for the σ₁ and σ₂ receptors and the vesicular acetylcholine transporter (VACHT) were determined using radioligand competition binding assays (σ₁ receptor: (+)-[³H]-pentazocine; σ₂ receptor: [³H]-1,3-di-*o*-tolylguanidine ([³H]DTG); VACHT: (-)-[³H]vesamicol) as reported previously.^{24–25} The results are provided in **Table 1**. In general, the introduction of a fluoroethoxy group maintained the nanomolar affinity of the indole-based analogs for σ₂ receptors (K_i(σ₂) = 1.79–5.23 nM) and increased the subtype selectivity (K_i(σ₁)/K_i(σ₂) = 56–708). The presence of the fluoroethoxy group at 4-position of the indole group led to higher subtype selectivity compared with the 5- or 6-position (**15** vs **19** and **21**, **16** vs **20** and **22**). The length of the carbon linker between the indole group and

the 6,7-dimethoxy-1,2,3,4-tetrahydroisoquinoline (or 5,6-dimethoxyisoindoline) moiety significantly influenced the subtype selectivity. The presence of four carbon units is favorable for σ_2 receptor affinity and subtype selectivity (**15** vs **13** and **17**, **16** vs **14** and **18**). Compounds with either the 5,6-dimethoxyisoindoline or 6,7-dimethoxy-1,2,3,4-tetrahydroisoquinoline moiety displayed similar affinity for σ_2 receptors (**13** vs **14**, **15** vs **16**, **21** vs **22**).

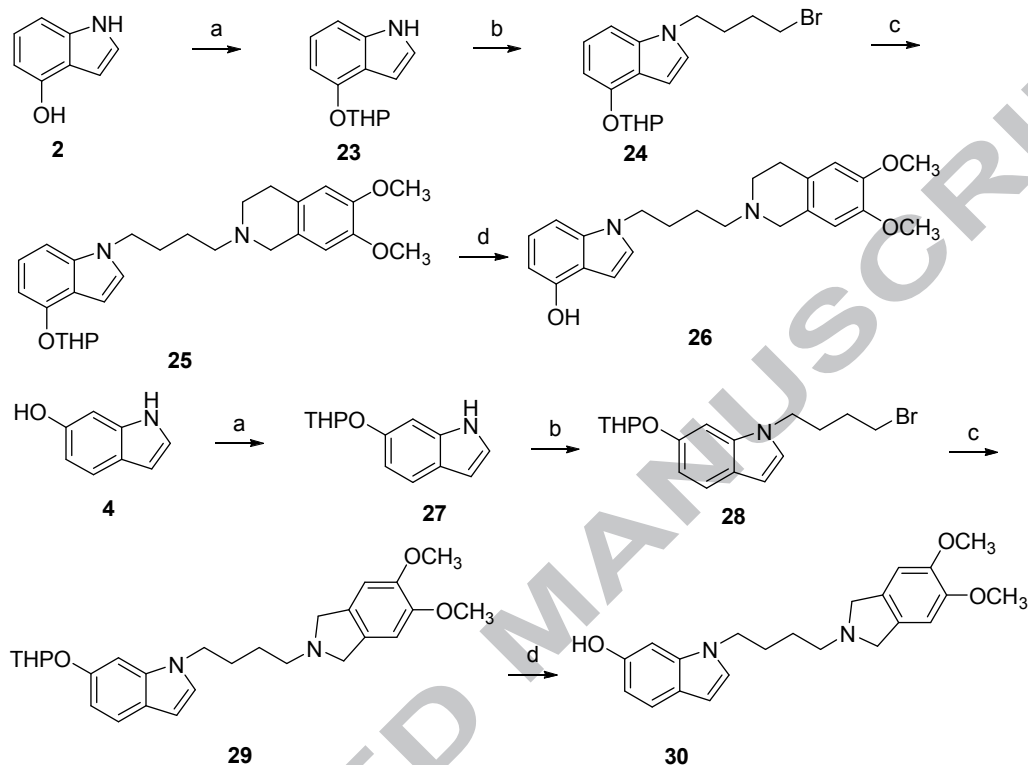
Considering the σ_2 receptor affinity, subtype selectivity, lipophilicity and positions of the fluoroethoxy substitution, compounds **15**, **16**, **20** and **21** were further tested for their VACHT affinity. All four compounds proved to be of high selectivity for σ_2 receptors over VACHT ($K_i(\text{VACHT})/K_i(\sigma_2) = 1488\text{--}19151$). The corresponding radioligands [^{18}F]**16** (fluoroethoxy group at the 4-position) and [^{18}F]**21** (fluoroethoxy group at the 6-position) were synthesized to investigate their binding and kinetic properties *in vivo*.

2.3 Radiochemistry.

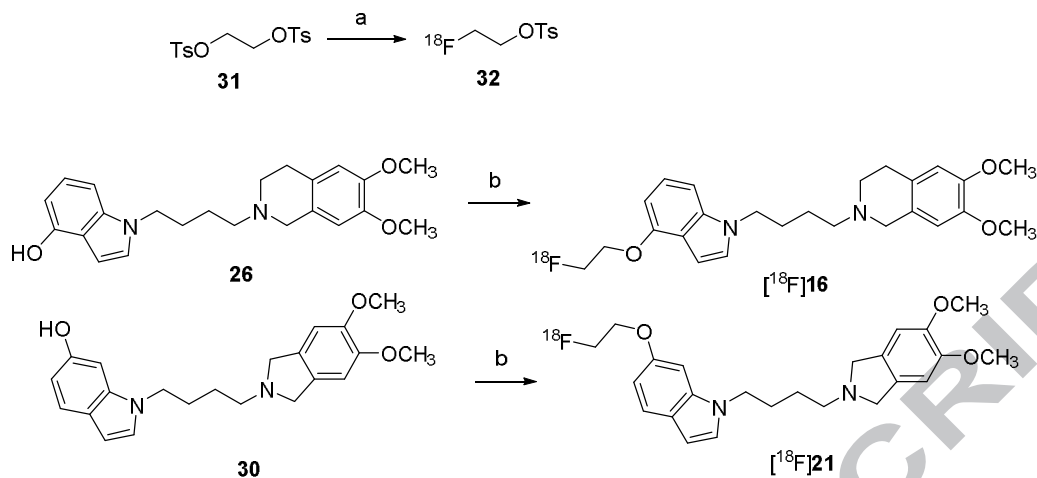
The precursors for radiolabelling were synthesized as outlined in **Scheme 2**. Protection of compound 4-hydroxyindole (**2**) or 6-hydroxyindole (**4**) with 3,4-dihydro-2*H*-pyran, followed by reaction with 1,4-dibromobutane provided compound **24** or **28**. *N*-Alkylation of 6,7-dimethoxy-1,2,3,4-tetrahydroisoquinoline and 5,6-dimethoxyisoindoline with **24** and **28** gave compounds **25** and **29**, respectively. Deprotection afforded compounds **26** and **30**. **Scheme 3** depicts the radiosynthesis of [^{18}F]**16** and [^{18}F]**21**, which were prepared by an efficient one-pot, two-step reaction sequence with a home-made automated synthesis module.²⁶ In the first step, 2,2'-(ethane-1,2-diyl)bis(4-methylbenzenesulfonate) reacted with Kryptofix 2.2.2/ $\text{K}^+[\text{}^{18}\text{F}]\text{F}^-$ complex to provide 2- $[\text{}^{18}\text{F}]$ fluoroethyl-1-tosylate. Alkylation of the precursors **26** and **30** with 2- $[\text{}^{18}\text{F}]$ fluoroethyl-1-tosylate (**32**) in the presence of Cs_2CO_3 gave radioligands [^{18}F]**16** and [^{18}F]**21**, respectively. After purification via semi-preparative HPLC, [^{18}F]**16** and [^{18}F]**21** were obtained in decay-corrected radiochemical yields of 10–15% ($n = 4$) and 16–21% ($n = 7$), respectively, and radiochemical purity (RCP) of > 99%. Specific activities were 29 ($n = 1$) and 26–34 GBq/ μmol ($n = 2$), respectively, for [^{18}F]**16** and [^{18}F]**21**.

In order to identify the radiotracer, [^{18}F]**16** and its reference compound **16**, and [^{18}F]**21** and its reference compound **21** were co-injected and their HPLC profiles assessed using acetonitrile and water containing 0.1% trifluoroacetic acid (TFA) (45:55, v/v) as mobile phase at a flow rate of 1 mL/min. The respective HPLC chromatograms are presented in **Figure 2**. The retention times were observed to be 13.18 and 13.27 min for **16** and [^{18}F]**16**, and 10.78

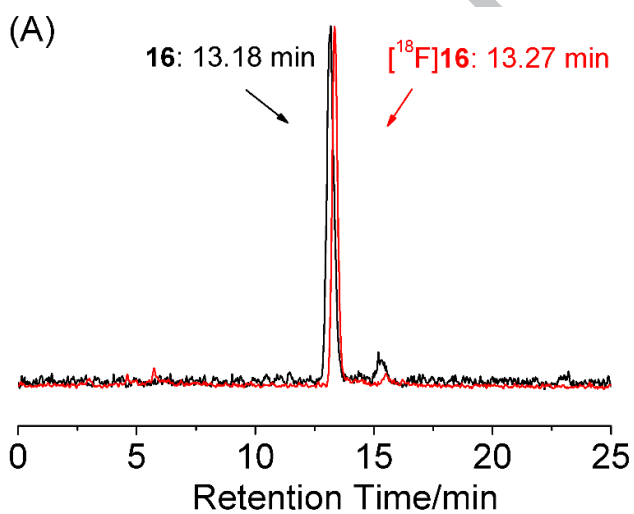
and 10.86 min for **21** and [^{18}F]**21**, respectively. The differences in retention times were in accordance with the time lag due to the volume and flow rate within the distance between the UV and radioactivity detectors of our HPLC system, thus indicating co-elution of the radiolabeled species with the unlabeled reference compounds.



Scheme 2. Reagents and conditions: (a) DHP, TFA, CH_2Cl_2 , 1 h, for **23**, 36%, and for **27**, 83%; (b) DMF, $\text{Br}(\text{CH}_2)_4\text{Br}$, KOH, TBAF, r.t., 2 h, for **24**, 72%, and for **28**, 47%; (c) K_2CO_3 , 6,7-dimethoxy-1,2,3,4-tetrahydroisoquinoline/5,6-dimethoxyisoindoline, 90°C , 6 h, for **25**, 69%, and for **29**, 83%; (d) HCl (1 mol/L), NaOH (1 mol/L), r.t., 1 h, for **26**, 33%, and for **30**, 33%.



Scheme 3. Radiosyntheses of [^{18}F]16 and [^{18}F]21. Reagents and conditions: (a) Kryptofix 2.2.2, Cs_2CO_3 , DMSO, 100 °C, 5 min; (b) **32**, DMSO, 140 °C, 25 min.



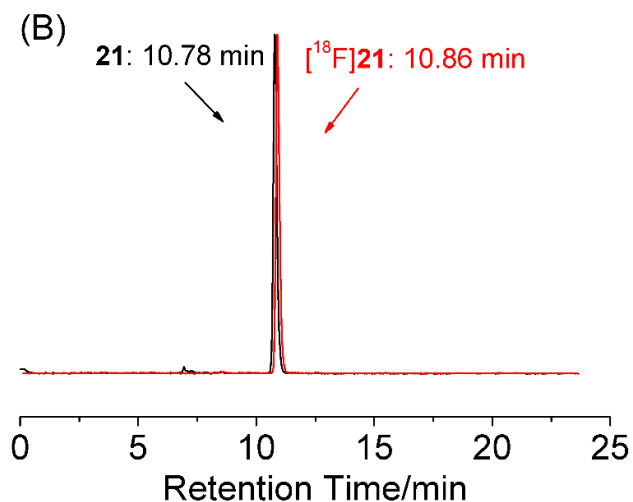


Figure 2. HPLC co-elution profiles of **16** and [¹⁸F]**16** (A), and **21** and [¹⁸F]**21** (B), with UV trace ($\lambda = 254$ nm) in black and radiotracer in red. Conditions: CH₃CN/H₂O (containing 0.1% TFA) = 45/55, v/v, flow rate = 1 mL/min.

2.4 Evaluation of the Radioligands.

2.4.1 Lipophilicity.

A shake-flask method was employed for the determination of the apparent distribution of the radiotracers as previously reported.²⁶ The log $D_{7.4}$ values were measured to be 2.35 ± 0.11 ($n = 3$) and 2.17 ± 0.13 ($n = 3$), respectively, for [¹⁸F]**16** and [¹⁸F]**21**.

2.4.2 *In vitro* stability.

The *in vitro* stability of [¹⁸F]**16** and [¹⁸F]**21** in saline was evaluated after 4 h of incubation at room temperature by measuring the RCP, which was maintained at > 99% as shown in **Figure 3**.

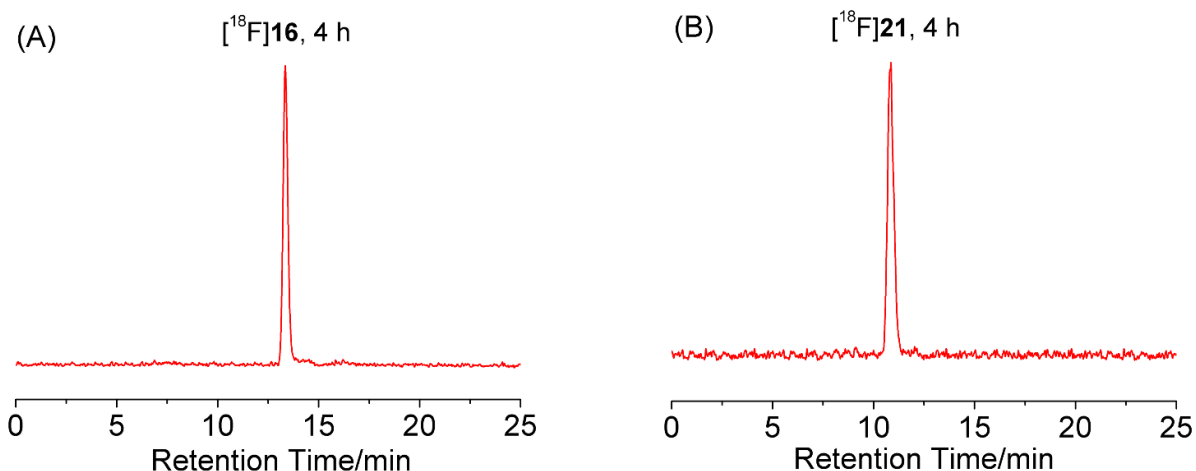


Figure 3. *In vitro* stability analysis: analytical radio-HPLC chromatograms of [^{18}F]16 and [^{18}F]21 in saline at room temperature at 4 h after synthesis.

2.4.3 Biodistribution studies in male ICR mice.

To evaluate the kinetics of [^{18}F]16 and [^{18}F]21, biodistribution studies were performed in male ICR mice at 2, 15, 30, 60 and 120 min after radiotracer injection. The results are summarized in **Tables 2** and **3**. Both [^{18}F]16 and [^{18}F]21 showed high initial brain uptake with $3.29 \pm 0.51\%$ ID/g and $4.55 \pm 0.43\%$ ID/g at 2 min, respectively, followed by a relatively fast clearance from the brain. The brain-to-blood ratios were highest at 15 min after injection, with 3.02 and 4.53 for [^{18}F]16 and [^{18}F]21, respectively. Relatively low accumulation of the radiotracers was observed in the bone, with $4.04 \pm 0.60\%$ ID/g and $5.46 \pm 1.42\%$ ID/g, respectively, at 120 min, indicating little defluorination of [^{18}F]16 and [^{18}F]21 *in vivo*.

To verify the binding specificity of [^{18}F]16 and [^{18}F]21 to σ_2 receptors *in vivo*, blocking studies were carried out by pre-administration of haloperidol ($2.7 \mu\text{mol/kg}$, 1 mg/kg , 0.1 mL) or compound **21** ($3 \mu\text{mol/kg}$, 1.2 mg/kg , 0.1 mL) at 5 min prior to radiotracer injection. Results are presented in **Figure 4**. For [^{18}F]16, pretreatment with haloperidol reduced the brain uptake by 26% ($p = 0.001$) and the brain-to-blood ratio by 35% ($p = 0.001$). Pretreatment with compound **21** reduced the brain uptake by 24% ($p = 0.001$) and the brain-to-blood ratio by 65% ($p < 0.001$). Moreover, pretreatment with compound **21** reduced the radiotracer uptake in the liver by 62% ($p < 0.001$) and the liver-to-blood ratio by 83% ($p < 0.001$). For [^{18}F]21, pretreatment with haloperidol reduced the brain uptake by 32% ($p < 0.001$) and the brain-to-blood ratio by 38% ($p = 0.002$). Pretreatment with compound **21** reduced the brain uptake by 21% ($p = 0.004$) and the brain-to-blood ratio by 68% ($p < 0.001$). Radiotracer uptake in the liver and the liver-to-blood ratio were reduced by 54% ($p < 0.001$).

and 81% ($p < 0.001$), respectively, by pretreatment with compound **21**. These data provide evidence for the binding specificity of [^{18}F]**16** and [^{18}F]**21** *in vivo*.

Table 2. Biodistribution of [^{18}F]**16** in male ICR mice^a

Organ	2 min	15 min	30 min	60 min	120 min
Blood	2.19 ± 0.25	1.00 ± 0.07	0.94 ± 0.17	1.04 ± 0.13	1.05 ± 0.07
Brain	3.29 ± 0.51	3.01 ± 0.24	2.19 ± 0.18	1.34 ± 0.13	1.01 ± 0.03
Heart	10.02 ± 1.76	3.21 ± 0.29	2.24 ± 0.34	1.56 ± 0.16	1.50 ± 0.11
Liver	8.33 ± 0.83	20.44 ± 2.56	24.26 ± 3.67	23.41 ± 3.09	17.12 ± 1.82
Spleen	4.56 ± 1.04	8.35 ± 1.01	7.59 ± 0.57	5.37 ± 0.65	3.76 ± 0.32
Lung	31.57 ± 4.67	9.77 ± 1.93	7.28 ± 0.9	3.67 ± 0.90	2.87 ± 0.30
Kidney	18.19 ± 2.33	16.77 ± 1.11	10.49 ± 0.84	6.63 ± 0.62	4.91 ± 0.49
Stomach ^b	7.31 ± 1.13	11.94 ± 0.81	14.5 ± 1.94	19.43 ± 2.35	20.97 ± 1.38
Small intestine ^b	1.25 ± 0.22	2.92 ± 0.44	1.98 ± 0.21	3.44 ± 1.15	3.83 ± 0.26
Muscle	4.08 ± 0.85	2.79 ± 0.33	1.78 ± 0.38	1.25 ± 0.12	1.05 ± 0.03
Bone	2.12 ± 0.40	3.77 ± 0.20	4.47 ± 0.70	4.53 ± 0.57	4.04 ± 0.60
Brain/blood	1.50	3.02	2.37	1.30	0.96

^aData are expressed as percentage of injected dose per gram (% ID/g), means ± SD, n = 5.

^bPercentage of injected dose per organ.

Table 3. Biodistribution of [^{18}F]**21** in male ICR mice^a

Organ	2 min	15 min	30 min	60 min	120 min
Blood	2.15 ± 0.23	0.75 ± 0.04	0.63 ± 0.09	0.54 ± 0.06	0.49 ± 0.04
Brain	4.55 ± 0.43	3.39 ± 0.29	2.28 ± 0.16	1.14 ± 0.07	0.97 ± 0.17
Heart	9.01 ± 0.83	2.60 ± 0.30	1.39 ± 0.55	1.14 ± 0.26	1.13 ± 0.10
Liver	8.87 ± 0.91	23.30 ± 0.98	31.60 ± 3.93	29.66 ± 2.04	26.24 ± 4.00
Spleen	6.06 ± 1.44	8.60 ± 0.29	8.26 ± 1.63	5.32 ± 0.44	4.11 ± 0.34
Lung	39.54 ± 8.12	9.25 ± 1.52	6.23 ± 0.94	5.12 ± 1.65	3.11 ± 0.64
Kidney	17.77 ± 1.91	11.07 ± 0.86	6.83 ± 0.90	4.26 ± 0.37	3.87 ± 0.25
Stomach ^b	7.33 ± 0.57	12.77 ± 0.85	14.83 ± 1.33	16.62 ± 2.00	21.51 ± 2.60

Small intestine ^b	1.42 ± 0.15	2.64 ± 0.43	2.38 ± 0.39	2.44 ± 0.45	2.48 ± 0.78
Muscle	3.83 ± 0.38	2.23 ± 0.30	1.63 ± 0.16	0.92 ± 0.13	0.84 ± 0.05
Bone	3.46 ± 0.43	4.73 ± 0.43	5.66 ± 1.12	3.70 ± 0.74	5.46 ± 1.42
Brain/blood	2.12	4.53	3.67	2.12	2.02

^aData are expressed as percentage of injected dose per gram (% ID/g), means ± SD, n = 5

^bPercentage of injected dose per organ.

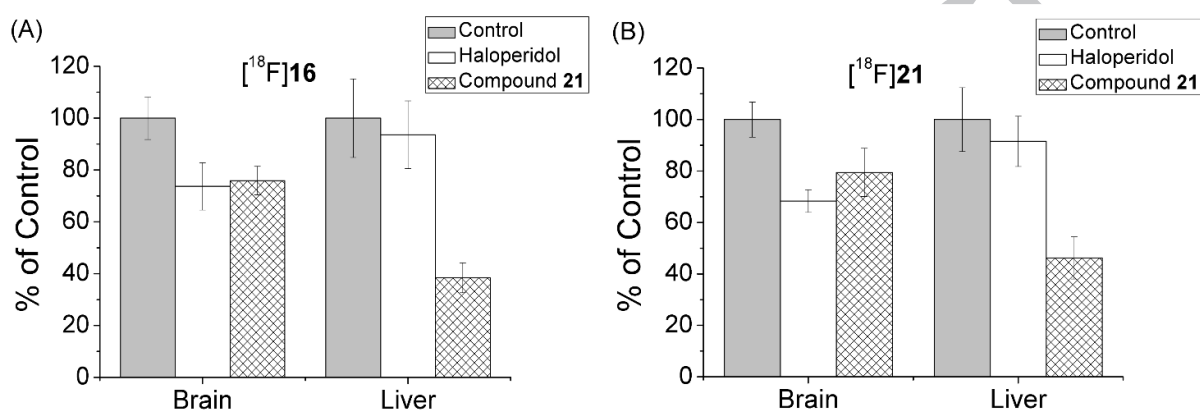


Figure 4. Effects of pretreatment with haloperidol (0.1 mL, 1.0 mg/kg) or compound **21** (0.1 mL, 3 μ mol/kg) on organ biodistribution of [¹⁸F]**16** and [¹⁸F]**21** at 30 min after intravenous injection. Student's *t* test (independent, two-tailed) was performed, and *p* < 0.05 (except for haloperidol in the liver).

2.4.4 Effect of P-gp on brain uptake of [¹⁸F]**16** and [¹⁸F]**21**.

P-glycoprotein (P-gp) is highly expressed at the blood-brain barrier (BBB) and restricts the brain entry of its substrates.²⁷ To test whether [¹⁸F]**16** and [¹⁸F]**21** are substrates for P-gp *in vivo*, cyclosporine A (50 mg/kg, 0.1 mL), an inhibitor of P-gp, was intravenously injected via the tail vein at 1 h prior to radiotracer injection. Radioligand distribution results are summarized in **Figure 5**. Cyclosporine A significantly increased the initial brain uptake of [¹⁸F]**16** and [¹⁸F]**21** by 201% and 51%, respectively, at 2 min postinjection. At the same time, the accumulation in the blood was maintained at the same level for [¹⁸F]**16** (2.19 ± 0.49% ID/g vs 2.13 ± 0.46% ID/g) and [¹⁸F]**21** (2.15 ± 0.23% ID/g vs 1.95 ± 0.38% ID/g). These data suggest that [¹⁸F]**16** and [¹⁸F]**21** may be substrates for P-gp.

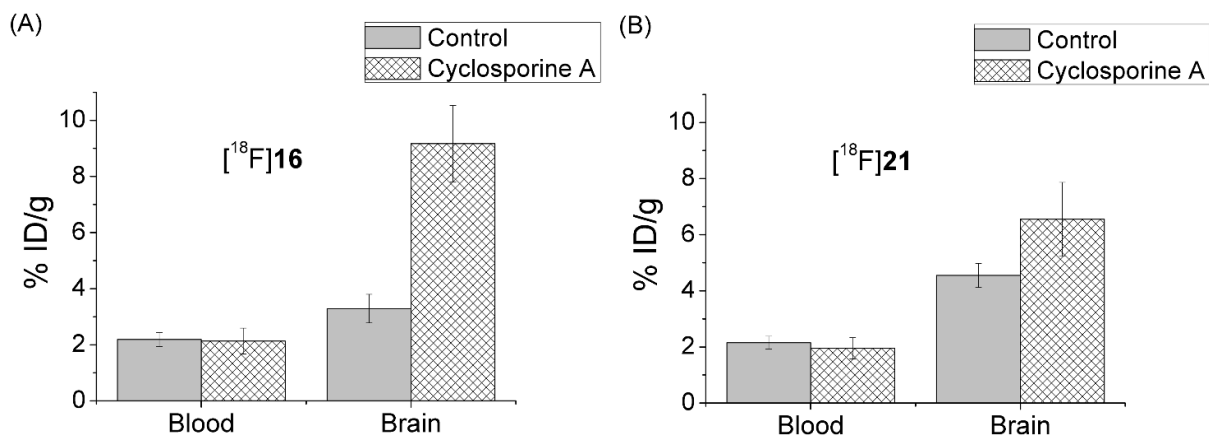


Figure 5. Effects of P-gp on brain uptake of [¹⁸F]16 and [¹⁸F]21 in mice. Student's *t* test (independent, two-tailed) was performed, and $p < 0.01$ for brain.

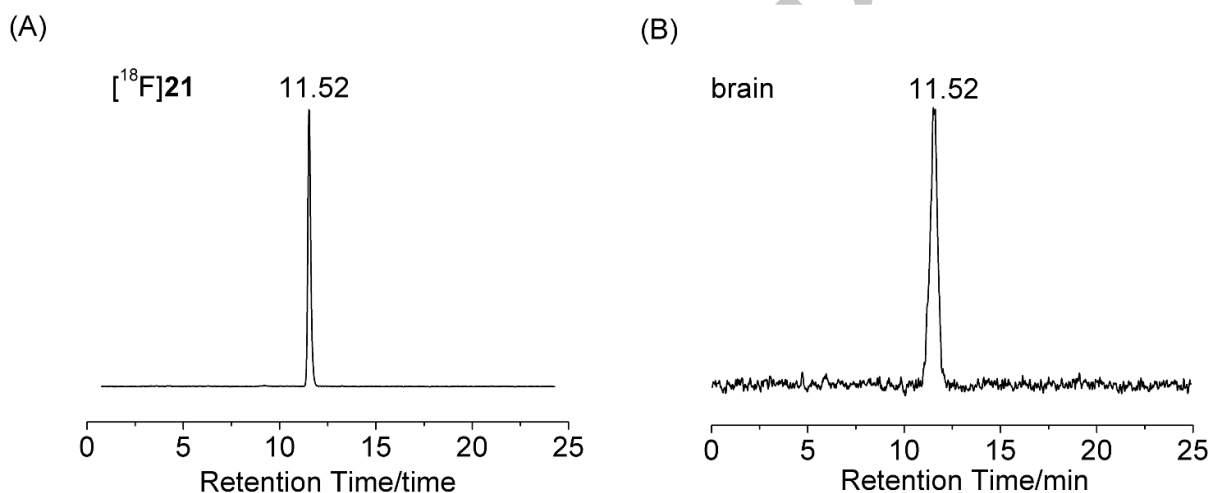


Figure 6. Analytical radio-HPLC chromatograms of the mouse brain extracts at 30 min after injection of [¹⁸F]21 (370 μ Ci, 0.1 mL, 7% ethanol in saline).

2.4.5 Analysis of radiometabolite in the brain.

A very important step in the development of brain imaging agent is to determine whether any radiometabolites of the radiotracer can enter the brain and confound the measurement of binding signal. Since the higher brain uptake and brain-to-blood ratio favors [¹⁸F]21, its radioactive species in the brain were analyzed in brain samples obtained from mice at 30 min after radiotracer injection, as previously reported.²⁶ The results are shown in **Figure 6**. In the brain, $\geq 95\%$ of the radioactivity signal represented the parent tracer [¹⁸F]21, indicating no entry of any radioactive metabolites into the brain.

3. DISCUSSION

The σ_2 receptor has been proposed as a potential biomarker for the proliferative status of solid tumors.⁸⁻¹² More recently it has also been suggested to play an important role in various brain disorders.¹³⁻¹⁵ and thus as a potential target for noninvasive imaging of neuronal/synaptic loss in neurodegenerative diseases using positron emission tomography (PET).²⁸ However, there is no suitable PET radiotracer available for imaging σ_2 receptors in the brain. In this study, we designed and synthesized a series of indole-based σ_2 receptor ligands in an effort to develop ¹⁸F-labeled radiotracers with high affinity, selectivity and suitability for imaging the σ_2 receptors in brain.

In vitro binding assays showed that these new compounds with fluoroethoxy moiety (**13–22**) possessed nanomolar affinity for σ_2 receptors and high subtype selectivity. Moreover, compounds **15**, **16**, **20**, and **21** displayed extremely high selectivity for σ_2 receptors over VAcHT (>1000-fold). Among the indole-based analogues, compound **16** with a 6,7-dimethoxy-1,2,3,4-tetrahydroisoquinoline moiety and the fluoroethoxy group at 4-position of the indole ring displayed the highest subtype selectivity. Compound **21** with a 5,6-dimethoxyisoindoline moiety and the fluoroethoxy group at 6-position of the indole ring displayed nanomolar affinity for σ_2 receptors, >100-fold subtype selectivity, and >10000-fold selectivity for σ_2 vs. VAcHT. The corresponding radiotracers [¹⁸F]**16** and [¹⁸F]**21** were thus prepared for further *in vitro* and *in vivo* evaluation.

Radioligand [¹⁸F]**21** (log $D_{7.4}$ = 2.17) displayed lower lipophilicity than [¹⁸F]**16** (log $D_{7.4}$ = 2.35), consistent with the lower lipophilicity of the 5,6-dimethoxyisoindoline moiety. The log $D_{7.4}$ values of both [¹⁸F]**16** and [¹⁸F]**21** are within the desirable range (log D = 1–3) for good BBB permeability required for brain imaging probes.²⁹ Both [¹⁸F]**16** and [¹⁸F]**21** also displayed excellent stability *in vitro*.

In biodistribution studies in mice, [¹⁸F]**16** (3.29 % ID/g at 2 min) and [¹⁸F]**21** (4.55 % ID/g at 2 min) showed higher initial brain uptake levels than the previously reported σ_2 radioligand [¹⁸F]ISO-1 (0.76 % ID/g at 2 min).²⁰ The brain-to-blood activity ratios of [¹⁸F]**16** and [¹⁸F]**21** at 15 min after injection were also high. In addition, pretreatment with haloperidol and compound **21** significantly reduced radiotracer accumulation in the brain and liver, providing evidence for specific binding of [¹⁸F]**16** and [¹⁸F]**21** to σ_2 receptors *in vivo*.

Ex vivo experiments were conducted to determine whether [¹⁸F]**16** and [¹⁸F]**21** are potential substrates for P-gp, as P-gp is highly expressed at the BBB and actively transports different lipophilic drugs out of the brain capillary endothelial cells. Pretreatment with the

P-gp inhibitor cyclosporine A at 60 min prior to radiotracer injection increased brain uptake of [^{18}F]16 and [^{18}F]21 by approximately 2.0-fold and 0.5-fold, respectively, while levels in the blood were not changed. These data indicate that [^{18}F]16 and [^{18}F]21 may be substrates for P-gp. The relatively lower initial brain uptakes of [^{18}F]16 and [^{18}F]21 (less than 5 % ID/g) could be attributed to the observation that both compounds appear to be weak substrates for P-gp, which might limit their utility in translational imaging studies. However, it is well known that a substrate of P-gp is species dependent.³⁰⁻³¹ Evaluation of [^{18}F]16 and [^{18}F]21 in higher animal species is warranted to further investigate this point.

Another important aspect for a brain radiotracer is the absence of radiometabolites able to cross the BBB into brain. [^{18}F]21 displayed higher brain uptake and brain-to-blood ratios than [^{18}F]16, and its radioactivity profile in the brain of male ICR mice was determined at 30 min after radioligand injection. The parent tracer [^{18}F]21 was found to be the only radioactive species in the mouse brain, indicating that radiometabolites generated in the periphery did not enter the brain.

4. Conclusion

We have successfully designed and synthesized a series of indole-based analogs with nanomolar affinity for σ_2 receptors and high subtype selectivity as well as high selectivity for σ_2 over VACHT. Radioligands [^{18}F]16 and [^{18}F]21 displayed suitable lipophilicity and high stability *in vitro*. Biodistribution results in ICR mice indicated that these two ^{18}F -labeled tracers displayed high brain uptake and high brain-to-blood ratios. Blocking studies confirmed specific binding of [^{18}F]16 and [^{18}F]21 to σ_2 receptors *in vivo*. *In vivo* metabolic studies indicated no presence of radioactive metabolites from [^{18}F]21 in the brain. Taken together, both of these two new radioligands appear to be suitable *in vivo* imaging agents for the σ_2 receptors and further development is warranted.

5. Experimental section

5.1. General method

All the chemicals or reagents were obtained from commercial suppliers without further purification. All synthesized compounds were monitored by thin-layer chromatography (TLC) on silica gel. ^1H NMR spectra were recorded on a Bruker Avance III (400 MHz) NMR spectrometer in CDCl_3 solutions at room temperature and with tetramethylsilane (TMS) as an internal standard. ^{13}C NMR spectra were recorded on a Bruker Avance III (100 MHz) NMR spectrometer. Chemical shifts (δ) are reported in ppm downfield from TMS and

coupling constants (J) in Hertz (Hz). Mass spectra were acquired on a Quattro micro API ESI/MS instrument (Waters, USA). High-resolution mass spectrometry (HRMS) was performed on a LCT Premier XE ESI-TOF mass spectrometer (Waters, USA). High performance liquid chromatography analysis and purification were performed on a Waters 600 system (Waters Corporation, USA) equipped with a Waters 2489 UV-VIS detector and a Raytest Gabi NaI (TI) scintillation detector (Raytest, Germany). Samples were separated on an Agela Venusil MP C18 column (250 × 4.6 mm, 5 μm) using 40% acetonitrile (containing 0.1% trifluoroacetic acid, TFA) and 60% water (containing 0.1% TFA) as mobile phase at a flow rate of 4 mL/min. Samples were analyzed using 45% acetonitrile (containing 0.1% TFA) and 55% water (containing 0.1% TFA) as mobile phase at a flow rate of 1 mL/min.

Normal male ICR mice (22–24 g, 4–5 weeks) were purchased from Vital River Experimental Animal Technical Co., LTD. All procedures of the animal experiments were carried out according to the relevant laws and institutional guidelines. The protocol was approved by the Institutional Animal Care and Use Committee of Beijing Normal University.

5.2. Chemistry

5.2.1. 4-(2-fluoroethoxy)-indole (**5**)

Compound **2** (202.2 mg, 1.52 mmol) and 1-bromo-2-fluoroethane (347.6 mg, 2.74 mmol) were dissolved in CH₃CN (30 mL), followed by addition of K₂CO₃ (637.1 mg, 4.61 mmol). The mixture was heated under reflux and stirred at 90 °C for 6 h. After cooling and filtration, the solvent was removed under reduced pressure. The residue was purified by silica gel column chromatography (petroleum ether/ethyl acetate/triethylamine = 10:5:1, v/v/v) to afford **5** (249.9 mg, 92%) as a pale yellow solid, MP: 119.0–120.2 °C. ¹H NMR (400 MHz, CDCl₃): δ 8.16 (s, 1H, indole N-H), 7.13–7.04 (m, 3H, Ar-H), 6.71–6.69 (m, 1H, Ar-H), 6.52 (dd, J = 7.5, 0.6 Hz, 1H, Ar-H), 4.83 (dt, J = 47.4, 4.2 Hz, 2H, F-CH₂), 4.38 (dt, J = 27.6, 4.3 Hz, 2H, O-CH₂). ESI-MS, [M+H]⁺: m/z = 180.2.

5.2.2. 5-(2-fluoroethoxy)-indole (**6**)

The procedure described for the synthesis of **5** was applied to compound **3** (215.8 mg, 1.62 mmol), 1-bromo-2-fluoroethane (400.2 mg, 3.15 mmol) and K₂CO₃ (626.6 mg, 4.53 mmol) to afford **6** (201.7 mg, 69%) as a pink oil. ¹H NMR (400 MHz, CDCl₃): δ 8.15 (s, 1H, indole N-H), 7.28–7.16 (m, 3H, Ar-H), 6.97 (dd, J = 8.8, 0.2 Hz, 1H, Ar-H), 6.55–6.53 (m, 1H, Ar-H), 4.80 (dt, J = 47.5, 4.2 Hz, 2H, F-CH₂), 4.27 (dt, J = 27.6, 4.2 Hz, 2H, O-CH₂). ESI-MS,

$[M+H]^+$: $m/z = 180.2$.

5.2.3. 6-(2-fluoroethoxy)-indole (**7**)

The procedure described for the synthesis of **5** was applied to compound **4** (500.0 mg, 3.76 mmol), 1-bromo-2-fluoroethane (732.5 mg, 5.77 mmol) and K_2CO_3 (1643.5 mg, 11.91 mmol) to afford **7** (470.1 mg, 70%) as a white solid. Mp: 92.3–93.9 °C. 1H NMR (400 MHz, $CDCl_3$): δ 8.05 (s, 1H, indole N-H), 7.53 (d, $J = 8.6$, 1H, Ar-H), 7.09 (s, 1H, Ar-H), 6.91 (s, 1H, Ar-H), 6.84 (d, $J = 8.6$, 1H, Ar-H), 6.50 (s, 1H, Ar-H), 4.78 (dt, $J = 47.5$, 4.0 Hz, 2H, F- CH_2), 4.25 (dt, $J = 27.9$, 4.1 Hz, 2H, O- CH_2). ESI-MS, $[M+H]^+$: $m/z = 180.2$.

5.2.4. 1-(3-bromopropyl)-4-(2-fluoroethoxy)-indole (**8**)

Tetrabutylammonium fluoride (85.0 mg, 0.33 mmol) and potassium hydroxide (278.6 mg, 4.97 mmol) were added to a solution of **5** (178.2 mg, 0.99 mmol) in DMF (2 mL). The reaction mixture was stirred at 0 °C for 1 h. Then 1,3-dibromopropane was added and the mixture was stirred for 1 h at room temperature. The solvent was removed. The residue was washed with saturated sodium chloride, extracted with dichloromethane and dried. The solvent was removed under reduced pressure. The residue was purified by silica gel chromatography (petroleum ether/ethyl acetate) = 10:1, v/v) to afford **8** (70.6 mg, 24%) as a yellow oil. 1H NMR (400 MHz, $CDCl_3$): δ 7.14 (t, $J = 8.0$ Hz, 1H, Ar-H), 7.07 (d, $J = 3.2$ Hz, 1H, Ar-H), 7.04 (d, $J = 8.3$ Hz, 1H, Ar-H), 6.66 (dd, $J = 3.1$, 0.7 Hz, 1H, Ar-H), 6.53 (d, $J = 7.7$ Hz, 1H, Ar-H), 4.84 (dt, $J = 47.5$, 4.2 Hz, 2H, F- CH_2), 4.38 (dt, $J = 27.7$, 4.3 Hz, 2H, O- CH_2), 4.32 (t, $J = 6.4$ Hz, 2H, indole N- CH_2), 3.30 (t, $J = 6.1$ Hz, 2H, Br- CH_2), 2.37–2.31 (m, 2H, CH_2).

5.2.5. 1-(4-bromobutyl)-4-(2-fluoroethoxy)-indole (**9**)

The procedure described for the synthesis of **8** was applied to compound **5** (290.1 mg, 1.62 mmol), tetrabutylammonium fluoride (84.6 mg, 0.33 mmol), potassium hydroxide (278.3 mg, 4.97 mmol) and 1,4-dibromobutane (1071.6 mg, 4.96 mmol) to afford **9** (376.6 mg, 74%) as a yellow oil. 1H NMR (400 MHz, $CDCl_3$): δ 7.10 (t, $J = 8.0$ Hz, 1H, Ar-H), 6.98–6.95 (m, 2H, Ar-H), 6.63 (d, $J = 3.1$ Hz, 1H, Ar-H), 6.49 (d, $J = 7.7$ Hz, 1H, Ar-H), 4.80 (dt, $J = 47.5$, 4.2 Hz, 2H, F- CH_2), 4.33 (dt, $J = 27.8$, 4.2 Hz, 2H, O- CH_2), 4.09 (t, $J = 6.8$ Hz, 2H, indole N- CH_2), 3.32 (t, $J = 6.5$ Hz, 2H, Br- CH_2), 2.00–1.92 (m, 2H, CH_2), 1.83–1.76 (m, 2H, CH_2). ESI-MS, $[M+H]^+$: $m/z = 314.0$.

5.2.6. 1-(5-bromopentyl)-4-(2-fluoroethoxy)-indole (**10**)

The procedure described for the synthesis of **8** was applied to compound **5** (193.4 mg, 1.08 mmol), tetrabutylammonium fluoride (83.9 mg, 0.32 mmol), potassium hydroxide (181.7 mg, 3.24 mmol) and 1,5-dibromopentane (744.4 mg, 3.24 mmol) to afford **10** (293.8 mg, 82%) as a yellow oil. ¹H NMR (400 MHz, CDCl₃): δ 7.12 (t, *J* = 8.0 Hz, 1H, Ar-H), 7.01–6.98 (m, 2H, Ar-H), 6.64 (d, *J* = 3.1 Hz, 1H, Ar-H), 6.51 (d, *J* = 7.7 Hz, 1H, Ar-H), 4.83 (dt, *J* = 47.5, 4.0 Hz, 2H, F-CH₂), 4.38 (dt, *J* = 28.0, 4.0 Hz, 2H, O-CH₂), 4.12 (t, *J* = 7.0 Hz, 2H, indole N-CH₂), 3.37 (t, *J* = 6.7 Hz, 2H, Br-CH₂), 1.90–1.82 (m, 4H, CH₂), 1.50–1.42 (m, 2H, CH₂).

5.2.7. 1-(4-bromobutyl)-5-(2-fluoroethoxy)-indole (**11**)

The procedure described for the synthesis of **8** was applied to compound **6** (201.0 mg, 1.12 mmol), tetrabutylammonium fluoride (113.7 mg, 0.44 mmol), potassium hydroxide (248.6 mg, 4.44 mmol) and 1,4-dibromobutane (1001.4 mg, 4.64 mmol) to afford **11** (162.6 mg, 46%) as a yellow oil. ¹H NMR (400 MHz, CDCl₃): δ 7.25 (d, *J* = 8.6 Hz, 1H, Ar-H), 7.13 (s, 1H, Ar-H), 7.08 (s, 1H, Ar-H), 6.94 (d, *J* = 7.8 Hz, 1H, Ar-H), 6.43 (s, 1H, Ar-H), 4.78 (d, *J* = 47.5 Hz, 2H, F-CH₂), 4.26 (d, *J* = 28.1 Hz, 2H, O-CH₂), 4.13 (t, *J* = 4.9 Hz, 2H, indole N-CH₂), 3.37 (t, *J* = 4.0 Hz, 2H, Br-CH₂), 1.99 (s, 2H, CH₂), 1.85 (s, 2H, CH₂). ESI-MS, [M+H]⁺: *m/z* = 314.0.

5.2.8. 1-(4-bromobutyl)-6-(2-fluoroethoxy)-indole (**12**)

The procedure described for the synthesis of **8** was applied to compound **7** (389.6 mg, 2.17 mmol), tetrabutylammonium fluoride (85.1 mg, 0.33 mmol), potassium hydroxide (258.6 mg, 4.62 mmol) and 1,4-dibromobutane (1432.1 mg, 6.63 mmol) to afford **12** (309.4 mg, 45%) as a yellow oil. ¹H NMR (400 MHz, CDCl₃): δ 7.51 (d, *J* = 8.5 Hz, 1H, Ar-H), 6.99 (d, *J* = 2.4 Hz, 1H, Ar-H), 6.86 (s, 1H, Ar-H), 6.81 (d, *J* = 8.6 Hz, 1H, Ar-H), 6.43 (d, *J* = 2.4 Hz, 1H, Ar-H), 4.80 (dt, *J* = 47.5, 3.8 Hz, 2H, F-CH₂), 4.28 (dt, *J* = 27.8, 3.9 Hz, 2H, O-CH₂), 4.09 (t, *J* = 6.8 Hz, 2H, indole N-CH₂), 3.38 (t, *J* = 6.5 Hz, 2H, Br-CH₂), 2.04–1.97 (m, 2H, CH₂), 1.90–1.82 (m, 2H, CH₂). ESI-MS, [M+H]⁺: *m/z* = 314.1.

5.2.9. 1-[3-(5,6-dimethoxyisoindolin-2-yl)butyl]-4-(2-fluoroethoxy)-indole (**13**)

Compound **8** (70.6 mg, 0.24 mmol) and 5,6-dimethoxyisoindoline (68.5 mg, 0.38 mmol) were dissolved in CH₃CN (30 mL), followed by addition of K₂CO₃ (138.8 mg, 1.00 mmol). The mixture was heated under reflux and stirred at 90 °C for 6 h. After cooling and filtration,

the solvent was removed under reduced pressure. The residue was purified by silica gel chromatography (petroleum ether/ethyl acetate/triethylamine) = 10:10:1, v/v/v) to afford **13** (56.8 mg, 59%) as a pale yellow oil. ^1H NMR (400 MHz, CDCl_3): δ 7.15–7.06 (m, 3H, Ar-H), 6.77 (s, 2H, Ar-H), 6.66 (dd, $J = 3.1, 0.5$ Hz, 1H, Ar-H), 6.52 (d, $J = 7.2$ Hz, 1H, Ar-H), 4.84 (dt, $J = 47.5, 4.2$ Hz, 2H, F- CH_2), 4.37 (dt, $J = 27.8, 4.3$ Hz, 2H, O- CH_2), 4.27 (t, $J = 6.7$ Hz, 2H, indole N- CH_2), 3.87 (s, 10H, O- CH_3 , Ar- CH_2 -N), 2.65 (t, $J = 6.7$ Hz, 2H, N- CH_2), 2.08–2.05 (m, 2H, CH_2). ^{13}C NMR (100 MHz, CDCl_3) δ (ppm): 152.43, 148.63, 137.94, 131.86, 127.08, 122.29, 119.61, 106.14, 103.84, 100.64, 98.63, 82.35 ($J = 169.2$, F- CH_2), 67.49 ($J = 20.6$, O- CH_2), 59.32, 56.34, 52.75, 44.12, 29.56. ESI-TOF MS calcd for $\text{C}_{23}\text{H}_{28}\text{FN}_2\text{O}_3$ $[\text{M}+\text{H}]^+$: 399.2084; found: 399.2076.

5.2.10.

2-{3-[4-(2-fluoroethoxy)-indol-1-yl]propyl}-6,7-dimethoxy-1,2,3,4-tetrahydroisoquinoline (**14**)

The procedure described for the synthesis of **13** was applied to compound **8** (59.7 mg, 0.20 mmol), 6,7-dimethoxy-1,2,3,4-tetrahydroisoquinoline (56.6 mg, 0.29 mmol) and K_2CO_3 (81.8 mg, 0.59 mmol) to afford **14** (39.4 mg, 48%) as a yellow oil. ^1H NMR (400 MHz, CDCl_3): δ 7.13–7.04 (m, 3H, Ar-H), 6.65 (dd, $J = 3.1, 0.3$ Hz, 1H, Ar-H), 6.62 (s, 1H, Ar-H), 6.53–6.50 (m, 2H, Ar-H), 4.84 (dt, $J = 47.5, 4.2$ Hz, 2H, F- CH_2), 4.37 (dt, $J = 27.8, 4.3$ Hz, 2H, O- CH_2), 4.24 (t, $J = 6.7$ Hz, 2H, indole N- CH_2), 3.86 (s, 3H, O- CH_3), 3.85 (s, 3H, O- CH_3), 3.52 (s, 2H, Ar- CH_2 -N), 2.85 (t, $J = 5.8$ Hz, 2H, Ar- CH_2), 2.67 (t, $J = 5.8$ Hz, 2H, N- CH_2), 2.43 (t, $J = 6.8$ Hz, 2H, N- CH_2), 2.09 (t, $J = 6.8$ Hz, 2H, CH_2). ^{13}C NMR (100 MHz, CDCl_3): δ 152.23, 147.57, 147.26, 137.75, 126.83, 126.70, 126.32, 122.04, 119.41, 111.49, 109.58, 103.68, 100.47, 98.44, 82.16 ($J = 169.2$, F- CH_2), 67.31 ($J = 20.5$, O- CH_2), 55.96, 55.93, 55.63, 54.63, 50.99, 44.03, 28.84, 27.63. ESI-TOF MS calcd for $\text{C}_{24}\text{H}_{30}\text{FN}_2\text{O}_3$ $[\text{M}+\text{H}]^+$: 413.2240; found: 413.2236.

5.2.11. 1-[4-(5,6-dimethoxyisoindolin-2-yl)butyl]-4-(2-fluoroethoxy)-indole (**15**)

The procedure described for the synthesis of **13** was applied to compound **9** (82.0 mg, 0.27 mmol), 5,6-dimethoxyisoindoline (73.6 mg, 0.41 mmol) and K_2CO_3 (206.1 mg, 1.49 mmol) to afford **15** (73.3 mg, 68%) as a yellow oil. ^1H NMR (400 MHz, CDCl_3): δ 7.11 (t, $J = 8.0$ Hz, 1H, Ar-H), 7.02 (dd, $J = 10.8, 5.7$ Hz, 2H, Ar-H), 6.72 (s, 2H, Ar-H), 6.64 (dd, $J = 3.1, 0.7$ Hz, 1H, Ar-H), 6.51 (d, $J = 7.6$ Hz, 1H, Ar-H), 4.83 (dt, $J = 47.4, 4.2$ Hz, 2H, F- CH_2), 4.37 (dt, $J = 27.7, 4.2$ Hz, 2H, O- CH_2), 4.16 (t, $J = 6.9$ Hz, 2H, indole N- CH_2), 3.89 (s, 4H, Ar- CH_2 -N), 3.85 (s, 6H, O- CH_3), 2.74 (t, $J = 7.4$ Hz, 2H, N- CH_2), 1.97–1.93 (m, 2H, CH_2),

1.64–1.60 (m, 2H, CH₂). ¹³C NMR (100 MHz, CDCl₃): δ 152.44, 148.57, 137.86, 131.86, 126.67, 122.24, 119.63, 106.09, 103.73, 100.64, 98.66, 82.34 (*J* = 170.2, F-CH₂), 67.43 (*J* = 20.7, O-CH₂), 59.37, 56.32, 55.70, 46.65, 28.27, 26.53. ESI-TOF MS calcd for C₂₄H₃₀FN₂O₃ [M+H]⁺: 413. 2240; found: 413. 2236.

5.2.12. 2-{4-[4-(2-fluoroethoxy)-indol-1-yl]butyl}-6,7-dimethoxy-1,2,3,4-tetrahydroisoquinoline (**16**)

The procedure described for the synthesis of **13** was applied to compound **9** (47.6 mg, 0.15 mmol), 6,7-dimethoxy-1,2,3,4-tetrahydroisoquinoline (51.2 mg, 0.26 mmol) and K₂CO₃ (123.5 mg, 0.89 mmol) to afford **16** (22.5 mg, 34%) as a yellow oil. ¹H NMR (400 MHz, CDCl₃): δ 7.09 (t, *J* = 8.0 Hz, 1H, Ar-H), 7.01 (dd, *J* = 7.3, 5.8 Hz, 2H, Ar-H), 6.63 (d, *J* = 3.0 Hz, 1H, Ar-H), 6.58 (s, 1H, Ar-H), 6.50 (d, *J* = 8.9 Hz, 2H, Ar-H), 4.83 (dt, *J* = 47.4, 4.2 Hz, 2H, F-CH₂), 4.37 (dt, *J* = 27.7, 4.2 Hz, 2H, O-CH₂), 4.14 (t, *J* = 7.0 Hz, 2H, indole N-CH₂), 3.83 (d, *J* = 3.0 Hz, 6H, O-CH₃), 3.48 (s, 2H, Ar-CH₂-N), 2.79 (t, *J* = 5.8 Hz, 2H, Ar-CH₂), 2.64 (t, *J* = 5.9 Hz, 2H, N-CH₂), 2.51–2.47 (m, 2H, N-CH₂), 1.93–1.88 (m, 2H, CH₂), 1.63–1.55 (m, 2H, CH₂). ¹³C NMR (100 MHz, CDCl₃): δ 151.75, 147.03, 146.72, 137.16, 126.13, 126.00, 125.71, 121.55, 118.96, 110.92, 109.04, 103.07, 99.98, 97.95, 81.65 (*J* = 170.3, F-CH₂), 66.81 (*J* = 21.0, O-CH₂), 57.18, 55.44, 55.42, 55.23, 50.55, 45.98, 28.19, 27.67, 24.07. ESI-TOF MS calcd for C₂₅H₃₂FN₂O₃ [M+H]⁺: 427.2397; found: 427.2394.

5.2.13. 1-[5-(5,6-dimethoxyisoindolin-2-yl)pentyl]-4-(2-fluoroethoxy)-indole (**17**)

The procedure described for the synthesis of **13** was applied to compound **10** (60.0 mg, 0.18 mmol), 5,6-dimethoxyisoindoline (85.5 mg, 0.47 mmol) and K₂CO₃ (129.6 mg, 0.94 mmol) to afford **17** (37.1 mg, 48%) as a yellow oil. ¹H NMR (400 MHz, CDCl₃): δ 7.11 (t, *J* = 8.0 Hz, 1H, Ar-H), 7.02 (t, *J* = 5.9 Hz, 2H, Ar-H), 6.74 (s, 2H, Ar-H), 6.64 (d, *J* = 3.1 Hz, 1H, Ar-H), 6.51 (d, *J* = 7.7 Hz, 1H, Ar-H), 4.83 (dt, *J* = 47.4, 4.2 Hz, 2H, F-CH₂), 4.37 (dt, *J* = 27.7, 4.2 Hz, 2H, O-CH₂), 4.10 (t, *J* = 7.0 Hz, 2H, indole N-CH₂), 3.90–3.85 (m, 10H, Ar-CH₂N, O-CH₃), 2.68 (t, *J* = 7.4 Hz, 2H, N-CH₂), 1.90–1.87 (m, 2H, CH₂), 1.60–1.58 (m, 2H, CH₂), 1.41 (t, *J* = 7.7 Hz, 2H, CH₂). ¹³C NMR (100 MHz, CDCl₃): δ 152.43, 148.58, 137.81, 131.94, 126.64, 122.19, 119.62, 106.07, 103.68, 100.66, 98.57, 82.23 (*J* = 169.2, F-CH₂), 67.42 (*J* = 20.7, O-CH₂), 59.40, 56.30, 56.09, 46.69, 30.37, 28.77, 24.91. ESI-TOF MS calcd for C₂₅H₃₂FN₂O₃ [M+H]⁺: 427.2391; found: 427.2390.

5.2.14.

2-{5-[4-(2-fluoroethoxy)-indol-1-yl]pentyl}-6,7-dimethoxy-1,2,3,4-tetrahydroisoquinoline (**18**)

The procedure described for the synthesis of **13** was applied to compound **10** (60.0 mg, 0.18 mmol), 6,7-dimethoxy-1,2,3,4-tetrahydroisoquinoline (75.3 mg, 0.39 mmol) and K_2CO_3 (123.8 mg, 0.89 mmol) to afford **18** (38.2 mg, 47%) as a yellow oil. 1H NMR (400 MHz, $CDCl_3$): δ 7.11 (t, $J = 8.0$ Hz, 1H, Ar-H), 7.01 (t, $J = 5.9$ Hz, 2H, Ar-H), 6.64 (dd, $J = 3.1, 0.5$ Hz, 1H, Ar-H), 6.59 (s, 1H, Ar-H), 6.51 (d, $J = 7.4$ Hz, 2H, Ar-H), 4.83 (dt, $J = 47.5, 4.2$ Hz, 2H, F- CH_2), 4.47 (dt, $J = 27.7, 4.2$ Hz, 2H, O- CH_2), 4.11 (t, $J = 7.1$ Hz, 2H, indole N- CH_2), 3.84 (s, 6H, O- CH_3), 3.53 (s, 2H, Ar- CH_2 -N), 2.81 (t, $J = 5.8$ Hz, 2H, Ar- CH_2), 2.68 (t, $J = 5.9$ Hz, 2H, N- CH_2), 2.46 (t, $J = 7.4$ Hz, 2H, N- CH_2), 1.90–1.84 (m, 2H, CH_2), 1.65–1.58 (m, 2H, CH_2), 1.42–1.36 (m, 2H, CH_2). ^{13}C NMR (100 MHz, $CDCl_3$): δ 151.28, 146.56, 146.25, 136.66, 125.70, 125.52, 125.27, 121.06, 118.46, 110.48, 108.61, 102.54, 99.49, 97.43, 81.15 ($J = 170.3$, F- CH_2), 66.32 ($J = 21.0$, O- CH_2), 54.96, 54.93, 54.83, 50.08, 45.53, 29.21, 27.68, 25.88, 23.92. ESI-TOF MS calcd for $C_{26}H_{34}FN_2O_3$ $[M+H]^+$: 441.2547; found: 441.2545.

5.2.15. 1-[4-(5,6-dimethoxyisoindolin-2-yl)butyl]-5-(2-fluoroethoxy)-indole (**19**)

The procedure described for the synthesis of **13** was applied to compound **11** (80.0 mg, 0.26 mmol), 5,6-dimethoxyisoindoline (93.6 mg, 0.52 mmol) and K_2CO_3 (222.0 mg, 1.61 mmol) to afford **19** (101.8 mg, 94%) as a yellow solid. MP: 91.8–92.5 °C. 1H NMR (400 MHz, $CDCl_3$): δ 7.24 (s, 1H, Ar-H), 7.11–7.10 (m, 2H, Ar-H), 6.92 (d, $J = 8.8$ Hz, 1H, Ar-H), 6.72 (s, 2H, Ar-H), 6.41 (d, $J = 2.7$ Hz, 1H, Ar-H), 4.77 (dt, $J = 47.4, 4.0$ Hz, 2H, F- CH_2), 4.26 (dt, $J = 28.1, 4.0$ Hz, 2H, O- CH_2), 4.15 (t, $J = 6.9$ Hz, 2H, indole N- CH_2), 3.89 (s, 4H, Ar- CH_2 -N), 3.85 (s, 6H, O- CH_3), 2.74 (t, $J = 7.3$ Hz, 2H, N- CH_2), 1.97–1.93 (m, 2H, CH_2), 1.64–1.60 (m, 2H, CH_2). ^{13}C NMR (100 MHz, $CDCl_3$): δ 152.84, 148.57, 131.91, 131.80, 129.03, 128.65, 112.59, 110.39, 106.07, 104.40, 100.76, 82.42 ($J = 170.0$, F- CH_2), 68.37 ($J = 20.5$, O- CH_2), 59.36, 56.30, 55.69, 46.63, 28.27, 26.56. ESI-TOF MS calcd for $C_{24}H_{30}FN_2O_3$ $[M+H]^+$: 413.2240; found: 413.2238.

5.2.16. 2-{4-[5-(2-fluoroethoxy)-indol-1-yl]butyl}-6,7-dimethoxy-1,2,3,4-tetrahydroisoquinoline (**20**)

The procedure described for the synthesis of **13** was applied to compound **11** (80.0 mg, 0.26 mmol), 6,7-dimethoxy-1,2,3,4-tetrahydroisoquinoline (99.6 mg, 0.52 mmol) and K_2CO_3 (146.1 mg, 1.06 mmol) to afford **20** (85.2 mg, 77%) as a yellow oil. 1H NMR (400 MHz, $CDCl_3$): δ 7.24 (s, 1H, Ar-H), 7.11–7.08 (m, 2H, Ar-H), 6.90 (d, $J = 8.9$ Hz, 1H, Ar-H), 6.58 (s,

1H, Ar-H), 6.48 (s, 1H, Ar-H), 6.40 (d, $J = 2.7$ Hz, 1H, Ar-H), 4.77 (dt, $J = 47.4, 3.9$ Hz, 2H, F-CH₂), 4.25 (dt, $J = 28.0, 4.0$ Hz, 2H, O-CH₂), 4.14 (t, $J = 6.9$ Hz, 2H, indole N-CH₂), 3.84 (s, 3H, O-CH₃), 3.83 (s, 3H, O-CH₃), 3.53 (s, 2H, Ar-CH₂-N), 2.81 (s, 2H, Ar-CH₂), 2.70 (s, 2H, N-CH₂), 2.52 (t, $J = 7.2$ Hz, 2H, N-CH₂), 1.94–1.90 (m, 2H, CH₂), 1.64–1.61 (m, 2H, CH₂). ¹³C NMR (100 MHz, CDCl₃): δ 152.16, 147.04, 146.72, 131.22, 128.36, 127.98, 126.07, 125.69, 111.89, 110.91, 109.72, 109.02, 103.74, 100.05, 81.73 ($J = 170.0$, F-CH₂), 67.70 ($J = 20.4$, O-CH₂), 57.14, 55.44, 55.41, 55.23, 50.51, 45.95, 28.16, 27.67, 24.10. ESI-TOF MS calcd for C₂₅H₃₂FN₂O₃ [M+H]⁺: 427.2397; found: 427.2394.

5.2.17. 1-[4-(5,6-dimethoxyisoindolin-2-yl)butyl]-5-(2-fluoroethoxy)-indole (**21**)

The procedure described for the synthesis of **13** was applied to compound **12** (80.0 mg, 0.26 mmol), 5,6-dimethoxyisoindoline (86.2 mg, 0.48 mmol) and K₂CO₃ (148.6 mg, 1.08 mmol) to afford **21** (66.6 mg, 62%) as a yellow solid. MP: 105.7–106.8 °C. ¹H NMR (400 MHz, CDCl₃) δ (ppm): 7.51 (d, $J = 8.6$ Hz, 1H, Ar-H), 7.02 (d, $J = 3.0$ Hz, 1H, Ar-H), 6.87 (s, 1H, Ar-H), 6.81 (d, $J = 8.6$ Hz, 1H, Ar-H), 6.73 (s, 2H, Ar-H), 6.43 (d, $J = 3.0$ Hz, 1H, Ar-H), 4.75 (dt, $J = 47.5, 4.0$ Hz, 2H, F-CH₂), 4.25 (dt, $J = 28.0, 4.0$ Hz, 2H, O-CH₂), 4.12 (t, $J = 7.0$ Hz, 2H, indole N-CH₂), 3.89 (s, 4H, Ar-CH₂-N), 3.85 (s, 6H, O-CH₃), 2.75 (t, $J = 7.2$ Hz, 2H, N-CH₂), 1.97–1.92 (m, 2H, CH₂), 1.65–1.61 (m, 2H, CH₂). ¹³C NMR (100 MHz, CDCl₃): δ 154.31, 147.91, 136.06, 131.14, 126.63, 123.00, 121.04, 108.92, 105.41, 100.42, 94.37, 81.66 ($J = 170.3$, F-CH₂), 67.51 ($J = 20.4$, O-CH₂), 58.69, 55.63, 54.91, 45.71, 27.24, 25.77. ESI-TOF MS calcd for C₂₄H₃₀FN₂O₃ [M+H]⁺: 413.2240; found: 413.2239.

5.2.18. 2-{4-[5-(2-fluoroethoxy)-indol-1-yl]butyl}-6,7-dimethoxy-1,2,3,4-tetrahydroisoquinoline (**22**)

The procedure described for the synthesis of **13** was applied to compound **12** (150.0 mg, 0.48 mmol), 6,7-dimethoxy-1,2,3,4-tetrahydroisoquinoline (151.1 mg, 0.78 mmol) and K₂CO₃ (216.4 mg, 1.57 mmol) to afford **22** (188.9 mg, 92%) as a yellow solid. MP: 85.1–86.4 °C. ¹H NMR (400 MHz, CDCl₃): δ 7.51 (d, $J = 8.6$ Hz, 1H, Ar-H), 7.02 (d, $J = 3.0$ Hz, 1H, Ar-H), 6.82 (s, 1H, Ar-H), 6.80 (d, $J = 8.6$ Hz, 1H, Ar-H), 6.58 (s, 1H, Ar-H), 6.49 (s, 1H, Ar-H), 6.42 (d, $J = 2.9$ Hz, 1H, Ar-H), 4.75 (dt, $J = 47.4, 4.0$ Hz, 2H, F-CH₂), 4.25 (dt, $J = 27.9, 4.0$ Hz, 2H, O-CH₂), 4.10 (t, $J = 7.0$ Hz, 2H, indole N-CH₂), 3.84 (d, $J = 2.7$ Hz, 6H, O-CH₃), 3.52 (s, 2H, Ar-CH₂-N), 2.81 (t, $J = 5.4$ Hz, 2H, Ar-CH₂), 2.70 (t, $J = 5.1$ Hz, 2H, N-CH₂), 2.52 (t, $J = 7.3$ Hz, 2H, N-CH₂), 1.94–1.88 (m, 2H, CH₂), 1.67–1.60 (m, 2H, CH₂). ¹³C NMR (100 MHz,

CDCl₃): δ 154.31, 147.04, 146.73, 136.04, 126.65, 126.04, 125.66, 123.02, 121.04, 110.89, 109.00, 108.91, 100.42, 94.41, 81.66 ($J = 170.0$, FCH₂), 67.70 ($J = 20.5$, OCH₂), 57.10, 55.43, 55.41, 55.24, 50.49, 45.76, 28.16, 27.40, 24.06. ESI-TOF MS calcd for C₂₅H₃₂FN₂O₃ [M+H]⁺: 427.2397; found: 427.2396.

5.2.19. 4-[(tetrahydro-pyran-2-yl)oxy]-indole (**23**)

A mixture of **2** (108.2 mg, 0.81 mmol) and 3,4-dihydro-2*H*-pyran (189.6 mg, 2.25 mmol) in CH₂Cl₂ (25 mL) was added to TFA (19.9 mg, 0.14 mmol). The mixture was heated under reflux and stirred at 40 °C for 1 h. After cooling and filtration, the solvent was removed under reduced pressure. The residue was purified by silica gel chromatography (petroleum ether/ethyl acetate) = 20:1, v/v) to afford **23** (63.4 mg, 36%) as a white solid. MP: 63.4–64.9 °C. ¹H NMR (400 MHz, CDCl₃): δ 8.16 (s, 1H, indole N-H), 7.15–7.00 (m, 3H, Ar-H), 6.81–6.51 (m, 2H, Ar-H), 5.63 (t, $J = 3.1$ Hz, 1H, CH), 4.04–3.98 (m, 1H, O-CH₂A), 3.65–3.61 (m, 1H, O-CH₂B), 1.99–1.92 (m, 2H, CH₂), 1.72–1.53 (m, 4H, CH₂). ESI-MS, [M+H]⁺: $m/z = 218.1$.

5.2.20. 1-(4-bromobutyl)-4-[(tetrahydro-pyran-2-yl)oxy]-indole (**24**)

The procedure described for the synthesis of **8** was applied to compound **23** (210.0 mg, 0.97 mmol), tetrabutylammonium fluoride (109.6 mg, 0.42 mmol), potassium hydroxide (113.2 mg, 2.02 mmol) and 1,4-dibromobutane (645.9 mg, 2.99 mmol) to afford **24** (245.4 mg, 72%) as a yellow oil. ¹H NMR (400 MHz, CDCl₃): δ 7.09–6.52 (m, 5H, Ar-H), 5.65 (t, $J = 4.1$ Hz, 1H, CH), 4.16 (t, $J = 6.8$ Hz, 2H, indole N-CH₂), 4.06–3.99 (m, 1H, O-CH₂A), 3.68–3.62 (m, 1H, O-CH₂B), 3.39 (t, $J = 6.5$ Hz, 2H, Br-CH₂), 2.01–1.91 (m, 4H, CH₂), 1.89–1.63 (m, 6H, CH₂). ESI-MS, [M+H]⁺: $m/z = 352.1$.

5.2.21.

6,7-dimethoxy-2-(4-{4-[(tetrahydro-pyran-2-yl)oxy]-indol-1-yl}butyl)-1,2,3,4-tetrahydroisoquinoline (**25**)

The procedure described for the synthesis of **13** was applied to compound **24** (273.1 mg, 0.78 mmol), 6,7-dimethoxy-1,2,3,4-tetrahydroisoquinoline (222.5 mg, 1.15 mmol) and K₂CO₃ (897.9 mg, 6.50 mmol) to afford **25** (250.0 mg, 69%) as a yellow oil. ¹H NMR (400 MHz, CDCl₃): δ 7.13 (t, $J = 7.9$ Hz, 1H, Ar-H), 7.04 (dd, $J = 8.1, 6.0$ Hz, 2H, Ar-H), 6.81 (d, $J = 7.7$ Hz, 1H, Ar-H), 6.64–6.52 (m, 3H, Ar-H), 5.66 (s, 1H, CH), 4.16 (t, $J = 6.8$ Hz, 2H, indole

N-CH₂), 4.03–4.01 (m, 1H, O-CH₂A), 3.86 (s, 6H, O-CH₃), 3.66–3.64 (m, 1H, O-CH₂B), 3.51 (s, 2H, Ar-CH₂-N), 2.82 (t, *J* = 5.4 Hz, 2H, Ar-CH₂), 2.67 (t, *J* = 5.7 Hz, 2H, N-CH₂), 2.51 (t, *J* = 7.3 Hz, 2H, N-CH₂), 2.22–1.95 (m, 4H, CH₂), 1.93–1.59 (m, 6H, CH₂). ESI-MS, [M+H]⁺: *m/z* = 465.3.

5.2.22. 1-{4-[6,7-dimethoxy-3,4-dihydroisoquinolin-2(1*H*)-yl]butyl}-4-hydroxyindole (**26**)

To the solution of compound **25** (230.3 mg, 0.50 mmol) in THF (10 mL) was added HCl (1 mol/L, 30 mL). The mixture was stirred at 40 °C for 30 min, followed by addition of NaOH (1 mol/L, 35 mL). After cooling and filtration, the solvent was removed under reduced pressure. The residue was purified by silica gel chromatography (petroleum ether/ethyl acetate/triethylamine) = 5:10:1, v/v/v) to afford **26** (62.1 mg, 33%) as a yellow solid. MP: 166.6–167.8 °C. ¹H NMR (400 MHz, CDCl₃): δ 9.28 (s, 1H, indole O-H), 7.16 (d, *J* = 3.1 Hz, 1H, Ar-H), 6.88–6.86 (m, 2H, Ar-H), 6.62 (s, 1H, Ar-H), 6.56 (s, 1H, Ar-H), 6.44 (d, *J* = 3.1 Hz, 1H, Ar-H), 6.35 (dd, *J* = 5.2, 3.1 Hz, 1H, Ar-H), 4.11 (t, *J* = 6.9 Hz, 2H, indole N-CH₂), 3.67 (d, *J* = 2.1 Hz, 6H, O-CH₃), 3.36 (s, 2H, Ar-CH₂-N), 2.66 (t, *J* = 5.5 Hz, 2H, Ar-CH₂), 2.53 (t, *J* = 5.7 Hz, 2H, N-CH₂), 2.39 (t, *J* = 7.1 Hz, 2H, N-CH₂), 1.79–1.75 (m, 2H, CH₂), 1.47–1.43 (m, 2H, CH₂). ESI-TOF MS calcd for C₂₃H₂₉N₂O₃ [M+H]⁺: 381.2172; found: 381.2174.

5.2.23. 6-[(tetrahydro-pyran-2-yl)oxy]-indole (**27**)

The procedure described for the synthesis of **23** was applied to compound **4** (982.2 mg, 7.37 mmol), 3,4-dihydro-2*H*-pyran (1892.9 mg, 22.50 mmol) and TFA (220.2 mg, 1.53 mmol) to afford **27** (230.3 mg, 14%) as a white solid. MP: 55.1–56.6 °C. ¹H NMR (400 MHz, CDCl₃): δ 8.03 (s, 1H, indole N-H), 7.52 (d, *J* = 8.0 Hz, 1H, Ar-H), 7.15–7.09 (m, 2H, Ar-H), 6.90 (d, *J* = 8.0 Hz, 1H, Ar-H), 6.49–7.48 (m, 1H, Ar-H), 5.43 (t, *J* = 3.2 Hz, 1H, C-H), 4.03–3.97 (m, 1H, O-CH₂A), 3.64–3.60 (m, 1H, O-CH₂B), 2.01–1.88 (m, 2H, CH₂), 1.71–1.56 (m, 4H, CH₂). ESI-MS, [M+H]⁺: *m/z* = 218.1.

5.2.24. 1-(4-bromobutyl)-6-[(tetrahydro-pyran-2-yl)oxy]-indole (**28**)

The procedure described for the synthesis of **8** was applied to compound **27** (420.0 mg, 1.93 mmol), tetrabutylammonium fluoride (108.9 mg, 0.42 mmol), potassium hydroxide (220.2 mg, 3.93 mmol) and 1,4-dibromobutane (1248.4 mg, 5.78 mmol) to afford **28** (322.3 mg, 47%) as a yellow oil. ¹H NMR (400 MHz, CDCl₃): δ 6.99 (d, *J* = 3.2 Hz, 1H, Ar-H), 6.58–6.49 (m, 3H, Ar-H), 6.13 (d, *J* = 3.1 Hz, 1H, Ar-H), 5.35 (t, *J* = 3.4 Hz, 1H, CH), 4.25 (t,

$J = 6.7$, 2H, indole N-CH₂), 4.19–4.16 (m, 1H, O-CH₂A), 3.90–3.88 (m, 1H, O-CH₂B), 3.69 (t, $J = 11.3$ Hz, 2H, Br-CH₂), 2.60–2.45 (m, 6H, CH₂), 2.37–2.23 (m, 4H, CH₂). ESI-MS, [M+H]⁺: $m/z = 352.1$.

5.2.25. 1-[4-(5,6-dimethoxyisoindolin-2-yl)butyl]-6-[(tetrahydro-pyran-2-yl)oxy]-indole (**29**)

The procedure described for the synthesis of **13** was applied to compound **28** (208.9 mg, 0.59 mmol), 5,6-dimethoxyisoindoline (184.5 mg, 0.95 mmol) and K₂CO₃ (247.2 mg, 1.79 mmol) to afford **29** (230.3 mg, 86%) as a yellow oil. ¹H NMR (400 MHz, CDCl₃): δ 7.50 (d, $J = 8.6$ Hz, 1H, Ar-H), 7.06–7.02 (m, 2H, Ar-H), 6.89 (dd, $J = 8.6, 2.1$ Hz, 1H, Ar-H), 6.73 (s, 2H, Ar-H), 6.42 (d, $J = 3.1$ Hz, 1H, Ar-H), 5.44 (t, $J = 3.2$ Hz, 1H, C-H), 4.11 (t, $J = 7.0$ Hz, 2H, indole N-CH₂), 3.99–3.97 (m, 1H, O-CH₂A), 3.86 (s, 6H, O-CH₃), 3.84 (s, 4H, Ar-CH₂-N), 3.63–3.59 (m, 1H, O-CH₂B), 2.71 (t, $J = 4.0$ Hz, 2H, N-CH₂), 1.95–1.57 (m, 10H, CH₂).

5.2.26. 1-[4-(5,6-dimethoxyisoindolin-2-yl)butyl]-6-hydroxyindole (**30**)

The procedure described for the synthesis of **26** was applied to compound **29** (220.2 mg, 0.49 mmol), 1 mol/L HCl (30 mL) and 1 mol/L NaOH (35 mL) to afford **30** (60.0 mg, 33%) as a white solid. MP: 150.5–151.9 °C. ¹H NMR (400 MHz, CDCl₃): δ 7.44 (d, $J = 8.4$ Hz, 1H, Ar-H), 6.98 (d, $J = 3.2$ Hz, 1H, Ar-H), 6.82 (d, $J = 1.9$ Hz, 1H, Ar-H), 6.72 (s, 2H, Ar-H), 6.65 (dd, $J = 8.5, 2.2$ Hz, 1H, Ar-H), 6.41 (d, $J = 3.1$ Hz, 1H, Ar-H), 4.07 (t, $J = 6.9$ Hz, 2H, indole N-CH₂), 3.92 (s, 4H, Ar-CH₂-N), 3.85 (s, 6H, O-CH₃), 2.75 (t, $J = 8.0$ Hz, 2H, N-CH₂), 1.97–1.89 (m, 2H, CH₂), 1.69–1.62 (m, 2H, CH₂). ESI-TOF MS calcd for C₂₂H₂₇N₂O₃ [M+H]⁺: 367.2016; found: 367.2017.

5.3. *In vitro* radioligand competition studies

All the procedures for the radioligand competition studies for σ receptors and VACHT were previously described.²⁴⁻²⁵ Detailed procedures are provided in the Supporting Information.

5.4. Radiochemistry

The syntheses of radiotracers were performed in a home-made synthesis module.²⁶ Detailed procedures are provided in the Supporting Information. Specific activity was determined with a HPLC-based method. For animal experiments, the radiotracer was formulated as a saline solution containing no more than 7% ethanol.

5.5. Determination of log *D* value

The log *D* value of [¹⁸F]16 and [¹⁸F]21 was determined by measuring the distribution of the radiotracer between 1-octanol and potassium phosphate buffer (PBS, 0.05 mol/L, pH 7.4).²⁶ Detailed procedures are provided in the Supporting Information.

5.6. *In vitro* stability studies

The *in vitro* stability of [¹⁸F]16 and [¹⁸F]21 were evaluated by monitoring the radiochemical purity at different time points according to literature procedures.²⁶ Detailed procedures are provided in the Supporting Information.

5.7. Biodistribution studies

The biodistribution experiments were performed in normal male ICR mice (22–24 g, 4–5 weeks). Detailed procedures are provided in the Supporting Information.

5.8. Effect of P-gp on the Brain Uptake of [¹⁸F]16 and [¹⁸F]21 in Mice

To investigate the effect of P-gp on the brain uptake of [¹⁸F]16 and [¹⁸F]21, mice were injected via the tail vein with cyclosporine A (50.0 mg/kg, 0.1 mL) 60 min prior to radiotracer injection. Detailed information is provided in the Supporting Information.

5.9. *In vivo* metabolic stability of [¹⁸F]21

The *in vivo* metabolic fate of [¹⁸F]21 was performed in male ICR mice. Detailed procedures are provided in the Supporting Information.

Acknowledgements

Partial support of the studies by the German Research Foundation (DFG, Br 1360/13-1) and the National Natural Science Foundation of China (No. 21471019) is gratefully acknowledged.

Supplementary data

Supplementary data associated with this article can be found, in the online version.

References

1. Hellewell SB, Bruce A, Feinstein G, Orringer J, Williams W, Bowen WD. Rat liver and

kidney contain high densities of σ_1 and σ_2 receptors: characterization by ligand binding and photoaffinity labeling. *Eur J Pharmacol.* 1994; 268: 9-18.

2. Vilner BJ, de Costa BR, Bowen WD. Cytotoxic effects of sigma ligands: sigma receptor-mediated alterations in cellular morphology and viability. *J Neurosci.* 1995; 15: 117-134.

3. Bem WT, Thomas GE, Mamone JY, Homan SM, Levy BK, Johnson FE, Coscia CJ. Overexpression of σ receptors in nonneural human tumors. *Cancer Res.* 1991; 51: 6558-6562.

4. Vilner BJ, John CS, Bowen WD. Sigma-1 and sigma-2 receptors are expressed in a wide variety of human and rodent tumor cell lines. *Cancer Res.* 1995; 55: 408-413.

5. John CS, Vilner BJ, Geyer BC, Moody T, Bowen WD. Targeting sigma receptor-binding benzamides as *in vivo* diagnostic and therapeutic agents for human prostate tumors. *Cancer Res.* 1999; 59: 4578-4583.

6. van Waarde A, Rybczynska AA, Ramakrishnan NK, Ishiwata K, Elsinga PH, Dierckx RAJO. Sigma receptors in oncology: therapeutic and diagnostic applications of sigma ligands. *Curr Pharm Des.* 2010; 16: 3519-3537.

7. Megalizzi V, Le Mercier M, Decaestecker C. Sigma receptors and their ligands in cancer biology: overview and new perspectives for cancer therapy. *Med Res Rev.* 2012; 32: 410-427.

8. Mach RH, Smith CR, Al-Nabulsi I, Whirrett BR, Childers SR, Wheeler KT. σ_2 receptors as potential biomarkers of proliferation in breast cancer. *Cancer Res.* 1997; 57: 156-161.

9. Al-Nabulsi I, Mach RH, Wang LM, Wallen CA, Keng PC, Sten K, Childers SR, Wheeler KT. Effect of ploidy, recruitment, environmental factors, and tamoxifen treatment on the expression of sigma-2 receptors in proliferating and quiescent tumour cells. *Br J Cancer* 1999; 81: 925-933.

10. Wheeler KT, Wang LM, Wallen CA, Childers SR, Cline JM, Keng PC, Mach RH. Sigma-2 receptors as a biomarker of proliferation in solid tumours. *Br J Cancer* 2000; 82: 1223-1232.

11. Mach RH, Zeng C, Hawkins WG. The σ_2 receptor: a novel protein for the imaging and treatment of cancer. *J Med Chem.* 2013; 56: 7137-7160.

12. Sai KKS, Jones LA, Mach RH. Development of ^{18}F -labeled PET probes for imaging cell proliferation. *Curr Top Med Chem.* 2013; 13: 892-908.

13. Zhang H, Cuevas J. Sigma receptors inhibit high-voltage-activated calcium channels in rat sympathetic and parasympathetic neurons. *J Neurophysiol* 2002; 87: 2867-2879.

14. Vilner BJ, Bowen WD. Modulation of cellular calcium by sigma-2 receptors: release from

intracellular stores in human SK-N-SH neuroblastoma cells. *J Pharmacol Exp Ther.* 2000; 292: 900-911.

15. Cassano G, Gasparre G, Niso M, Contino M, Scalera V, Colabufo NA. F281, synthetic agonist of the sigma-2 receptor, induces Ca^{2+} efflux from the endoplasmic reticulum and mitochondria in SK-N-SH cells. *Cell Calcium* 2009; 45: 340-345.

16. Bezprozvanny I. Calcium signaling and neurodegenerative diseases. *Trends Mol Med.* 2009; 15: 89-100.

17. Izzo NJ, Xu J, Zeng C, Kirk MJ, Mozzoni K, Silky C, Rehak C, Yurko R, Look G, Rishton G, Safferstein H, Cruchaga C, Goate A, Cahill MA, Arancio O, Mach RH, Craven R, Head E, LeVine H, Spires-Jones TL, Catalano SM. Alzheimer's therapeutics targeting amyloid beta 1-42 oligomers II: Sigma-2/PGRMC1 receptors mediate Abeta 42 oligomer binding and synaptotoxicity. *PLoS One* 2014; 9: e111899.

18. Sahlholm K, Liao F, Holtzman DM, Xu J, Mach RH. Sigma-2 receptor binding is decreased in female, but not male, APP/PS1 mice. *Biochem Biophys Res Commun.* 2015; 460: 439-445.

19. Yi B, Sahn JJ, Ardestani PM, Evans AK, Scott LL, Chan JZ, Iyer S, Crisp A, Zuniga G, Pierce JT, Martin SF, Shamloo M. Small molecule modulator of sigma 2 receptor is neuroprotective and reduces cognitive deficits and neuroinflammation in experimental models of Alzheimer's disease. *J Neurochem.* 2017;140: 561-575.

20. Tu Z, Xu J, Jones LA, Li S, Dumstorff C, Vangveravong S, Chen DL, Wheeler KT, Welch MJ, Mach RH. Fluorine-18-labeled benzamide analogues for imaging the σ_2 receptor status of solid tumors with positron emission tomography. *J Med Chem.* 2007; 50: 3194-3204.

21. Dehdashti F, Laforest R, Gao F, Shoghi KI, Aft RL, Nussenbaum B, Kreisel FH, Bartlett NL, Cashen A, Wagner-Johnson N, Mach RH. Assessment of cellular proliferation in tumors by PET using ^{18}F -ISO-1. *J Nucl Med.* 2013; 54: 350-357.

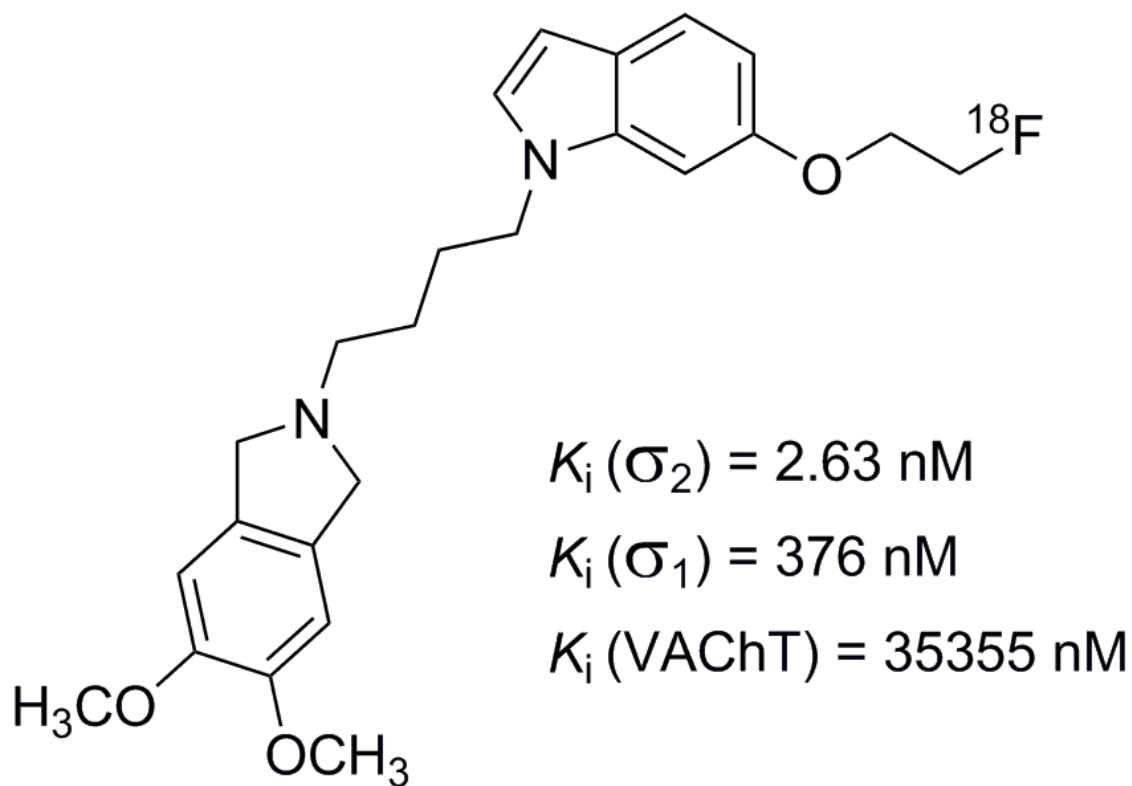
22. Shoghi KI, Xu J, Su Y, He J, Rowland D, Yan Y, Garbow JR, Tu Z, Jones LA, Higashikubo R. Quantitative receptor-based imaging of tumor proliferation with the sigma-2 ligand [^{18}F]ISO-1. *PLoS one* 2013; 8: e74188.

23. Mesangeau C, Amata E, Alsharif W, Seminerio MJ, Robson MJ, Matsumoto RR, Poupaert JH, McCurdy CR. Synthesis and pharmacological evaluation of indole-based sigma receptor ligands. *Eur J Med Chem.* 2011; 46: 5154-5161.

24. Fan C, Jia H, Deuther-Conrad W, Brust P, Steinbach J, Liu B. Novel $^{99\text{m}}\text{Tc}$ labeled σ receptor ligand as a potential tumor imaging agent. *Sci China Ser B* 2006; 49: 169-176.

25. Sorger D, Scheunemann M, Großmann U, Fischer S, Vercouille J, Hiller A, Wenzel B,

- Roghani A, Schliebs R, Brust P, Sabri O, Steinbach J. A new ^{18}F -labeled fluoroacetylmorpholino derivative of vesamicol for neuroimaging of the vesicular acetylcholine transporter. *Nucl Med Biol.* 2008; 35: 185-195.
26. Chen YY, Wang X, Zhang JM, Deuther-Conrad W, Zhang XJ, Huang Y, Li Y, Ye JJ, Cui MC, Steinbach J, Brust P, Liu BL, Jia HM. Synthesis and evaluation of a ^{18}F -labeled spirocyclic piperidine derivative as promising σ_1 receptor imaging agent. *Bioorg Med Chem.* 2014; 22: 5270-5278.
27. Kreisl WC, Liow JS, Kimura N, Seneca N, Zoghbi SS, Morse CL, Herscovitch P, Pike VW, Innis RB. P-glycoprotein function at the blood-brain barrier in humans can be quantified with the substrate radiotracer ^{11}C -N-desmethyl-loperamide. *J Nucl Med.* 2010; 51: 559-566.
28. Zeng C, Garg N, Mach RH. The PGRMC1 protein level correlates with the binding activity of a sigma-2 fluorescent probe (SW120) in rat brain cells. *Mol Imaging Biol.* 2016; 18: 172-179.
29. Patel S, Gibson R. In vivo site-directed radiotracers: a mini-review. *Nucl Med Biol.* 2008; 35: 805-815.
30. Yamazaki M, Neway WE, Ohe T, Chen I, Rowe JF, Hochman JH, Chiba M, Lin JH. In vitro substrate identification studies for P-glycoprotein-mediated transport: species difference and predictability of in vivo results. *J Pharmacol Exp Ther.* 2001; 296: 723-735.
31. Syvänen S, Lindhe O, Palner M, Kornum BR, Rahman O, Långström B, Knudsen GM, Hammarlund-Udenaes M. Species differences in blood-brain barrier transport of three positron emission tomography radioligands with emphasis on P-glycoprotein transport. *Drug Metab Dispos.* 2009; 37: 635-643.



ACCEPTED MANUSCRIPT